R. R. P.
6-1-84
(Restricted) Keep

6/84

NASA CR-174654

NASA 4-1-5-Z-F
WDL-TR10138
10 January 1984

FINAL REPORT

SPACECRAFT MULTIBEAM ANTENNA SYSTEM FOR 30/20 GHz

Contract No. NAS 3-22498
Submitted to:
NASA/Lewis Research Center
Cleveland, OH. 44135

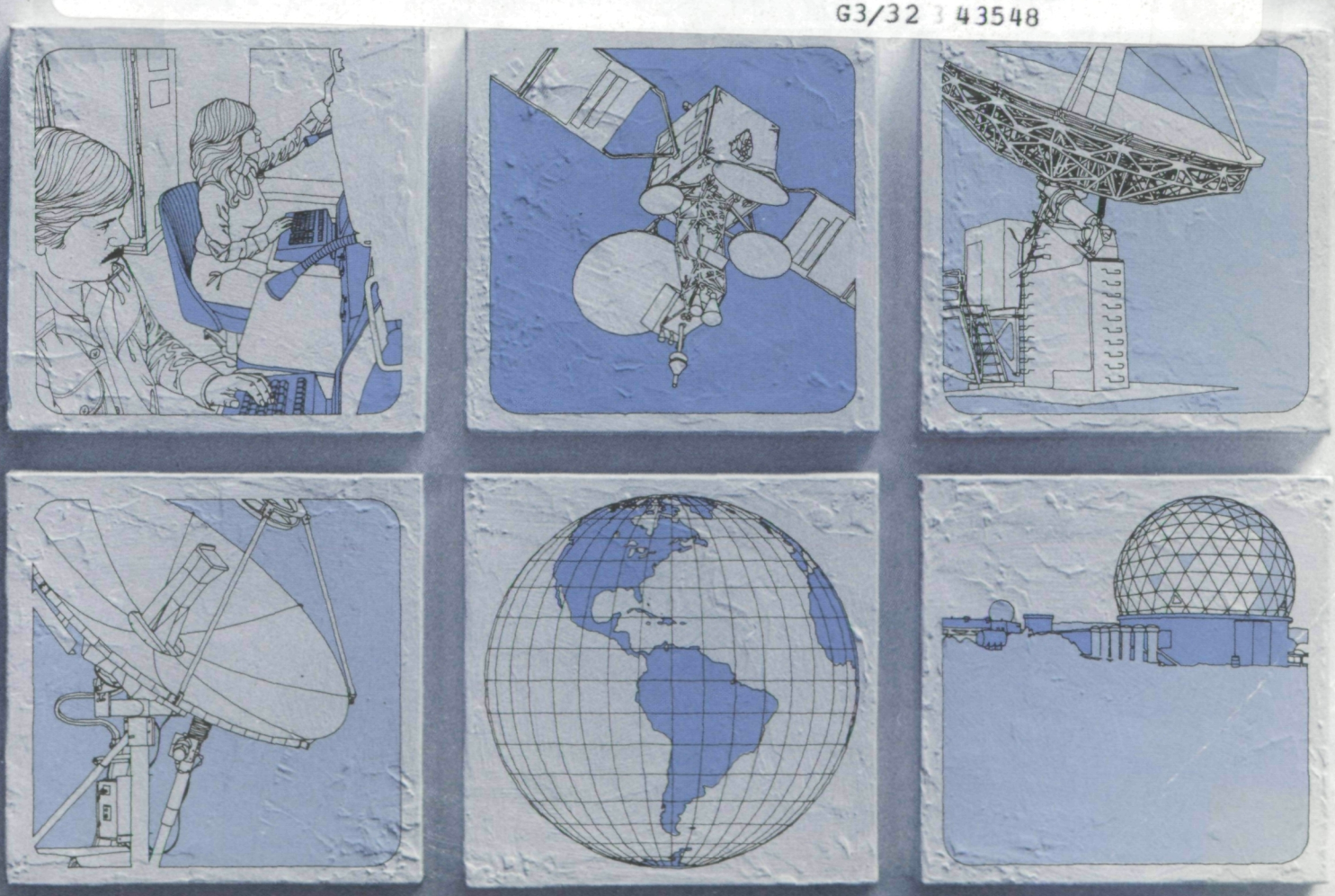

Ford Aerospace & Communications Corporation / Western Development Laboratories Division

NASA 4-1-5-Z-F
WDL-TR10138
10 January 1984

FINAL REPORT

SPACECRAFT MULTIBEAM ANTENNA SYSTEM FOR 30/20 GHz

Responsible Project Engineer: T. E. Roberts

FINAL REPORT

TABLE OF CONTENTS

LIST OF FIGURES

LIST OF TABLES

SPACECRAFT MULTIBEAM

ANTENNA SYSTEM FOR 30/20 GHz

FINAL REPORT

This final report describes the major technical tasks that led to the definitions of Operational and Demonstration Multiple Beam Antenna Flight Systems and a Proof of Concept Model. Features of the POC Model and its measured performance are presented in detail.

Similar MBA's are proposed for transmitting and receiving with the POC Model representing the 20 GHz transmitting antenna. This POC MBA is a dual shaped-surface reflector system utilizing a movable feed array to simulate complete CONUS coverage. The beam forming network utilizes ferrite components for switching from one beam to another.

Measured results for components, subsystems and the complete MBA confirm the feasibility of the approach and also show excellent correlation with calculated values.

Contract No. NAS 3-22498
Submitted to:

NASA/Lewis Research Center
Cleveland, OH. 44135

1.0 Background and Schedule

The statement of work, Exhibit "A" of the contract, which presents background, objective, approach, scope, specific tasks, requirements, and schedule in detail, has provided basic program direction throughout the life of the contract. Much of the following is essentially an abbreviated summary of the SOW.

The continuing rapid growth of satellite communications requires the use of additional frequency bands, and the 30/20 GHz frequencies are the next higher allocated bands. NASA-sponsored communications research and development programs are aimed at the development of customer premise and trunk service with frequency reuse. This present contract effort has therefore been directed to the development and demonstration of the necessary antenna technology to permit maximum frequency reuse.

The objective has been to perform technology development in the area of multiple beam antenna systems for geostationary communications satellites including design, construction, and testing of a proof of concept model. The approach has been to formulate and analyze multiple beam antenna systems, assess the impact of downstream technology, design, construct, and test a laboratory model to establish proof of concept for the proposed system.

The MBA specifications are given in Table 1.1 for the operational and demonstration systems, and the goals for Tasks I and II were to define operational and demonstration systems that meet these specifications. Specifications for the POC model are the same except for the number of beams, and the goals of Tasks V to VIII were to define, design, build and test a model that meets these.

All 18 trunk beams for major cities utilize the same 500 MHz frequency band, and all 6 scan beams utilize another 500 MHz frequency band.

The work scope is precisely specified by the SOW tasks, and the entire program was carried out within the original scope definitions except for Task 12, Flight Development Plan for Flight Hardware, which was deleted and MOD 12, which was added. Figure 1.1 displays the technical tasks and the performance schedule for each.

Table 1.1 Specifications for Multiple Beam Antenna

		TRUNKING Fixed Beam Reflector or Lens Type	CUSTOMER-PREMISE-SERVICE Scanning Beam Reflector or Lens Type
Antenna Size		Shuttle Compatible	
Downlink Freq. GHz		17.7-20.2	17.7-20.2
Uplink Freq.		27.5-30.0	27.5-30.0
Operational Beams		18	6 Trans & 6 Receive
Demonstration Beams		10 (any 6 active)	2 Trans & 2 Receive
Gain (dB)	-20 GHz	53	53
	-30 GHz	56	53
Bandwidth (MHz)		500	500
Polarization		Dual Linear	Dual Linear
C/I Performance (dB)		>30	>30
Pointing Accuracy (degrees)			
Pitch/Roll		<0.02	<0.02
Yaw		<0.40	<0.40

The amount of planned work for each task was a reasonably good approximation of the actual work carried out except for Task VII, Fabrication, which was strongly impacted by the design and fabrication requirements of the shaped surface reflectors to meet the specified surface tolerences and structural deflections. Extra cost and additional time was required to complete this task.

Task	1980	1981	1982	1983
1. Operational Design Concepts	----			
2. Demonstration Design Concepts	-			
3. POC Model Recommendation	-----			
4. Breadboard Component Development	----	----------		
5. POC Model Development Plan and Specification		----------		
6. POC Model Design and Test Plan		----------	----------	
7. POC Model Fabrication			----------	
8. POC Model Testing			----------	
MOD 12 Reliability Assessment			---	

Figure 1.1 Technical Task Schedule

2.0 System Description

Initial studies were conducted wherein a number of potential MBA system configurations were compared in a variety of spacecraft configurations for feasibility. The selected MBA system consists of two dual reflectors array fed antennas, one for receiving at 30 GHz and one for transmitting at 20 GHz, as shown in Figure 2.1. The 20 GHz transmitting antenna aperture is 13.5 feet in diameter which provides nominal half power beamwidth of 0.25 degrees and gain of 55dB.

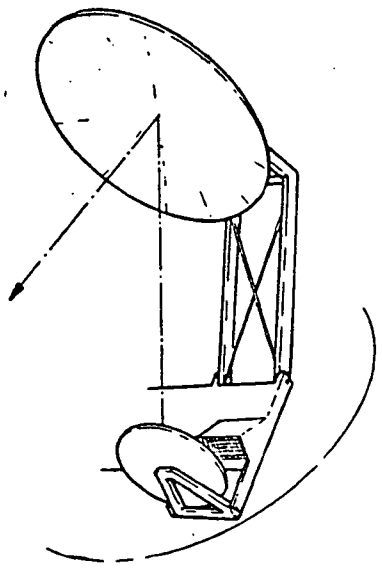

Figure 2.1 Dual Reflector MBA System

2.1 Operational Satellite Concept

The selected scan beam layout is for six contiguous rectangular sectors with long dimensions running North-South across CONUS as shown in Figure 2.2. The electric polarization alternates from horizontal to vertical for adjoining sectors thereby eliminating copol interference between adjoining sectors. The required close-in crosspol isolation is therefore 30 dB, but the copol isolation of 30 dB is required only for angles greater than 1.1 degrees from beam peak. (See Figure 2.3).

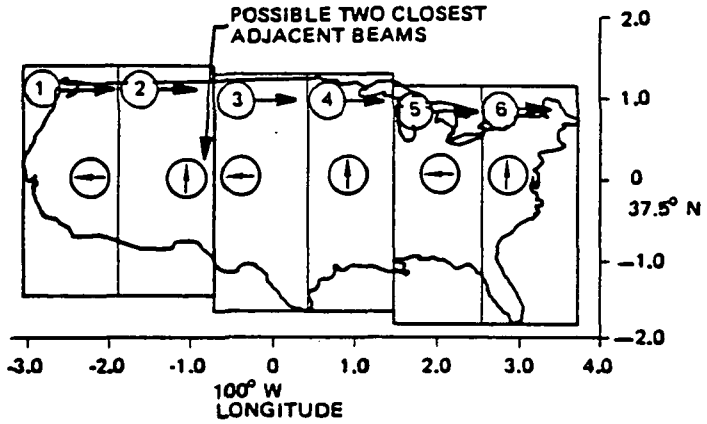

Figure 2.2 CPS Scan Beam Coverages for CPS System (The arrow indicates polarization)

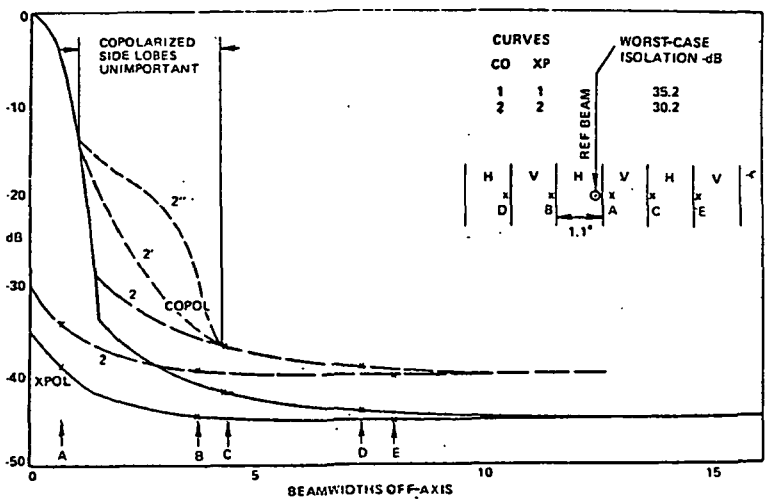

Figure 2.3 Scanning CPS Isolation

The complete feedhorn array, overlayed by a CONUS map, and showing the 18 trunk arrays and 6 scan sectors is displayed in Figure 2.4. The most critical areas for interference are for the trunk beams in the areas of Buffalo-Cleveland, Chicago-St. Louis, and Boston-New York-Washington. Good crosspol discrimination can provide the necessary isolation from New York. Isolation from between Washington and Boston depends on copol discrimination. Since these two cities are about 0.7 spacecraft degrees apart, however, the copol isolation should be expected to be considerably greater than 30dB.

After having selected the general form of the multiple beam antenna system, the next task was to refine the design to more specifically define the array and reflectors to meet the specified angular coverage. The considerations leading to the final selection are discussed below beginning with the optics design.

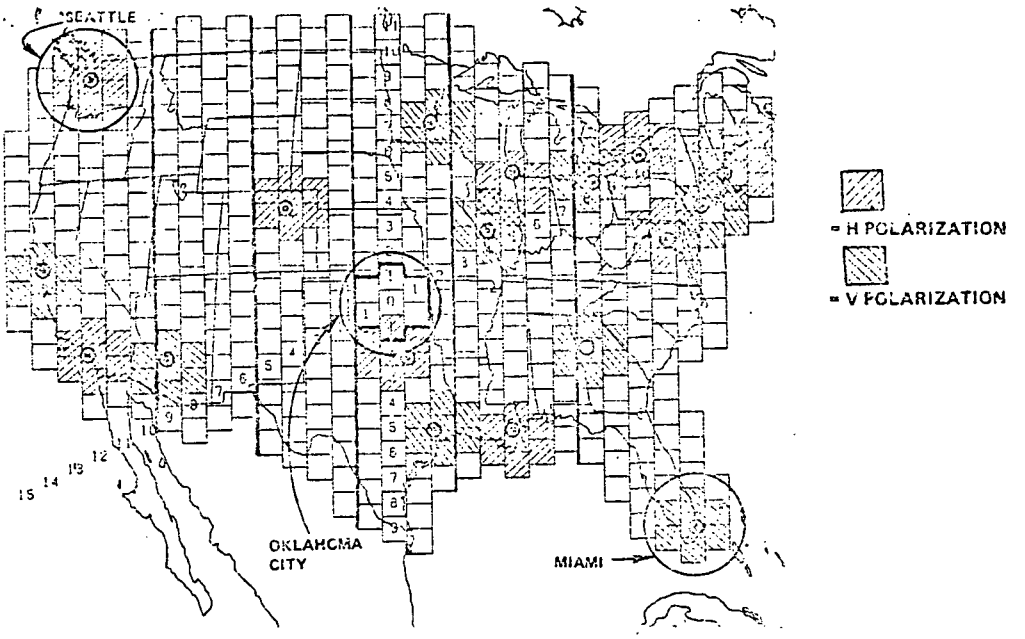

Figure 2.4 CONUS Feed Array Showing Scan Sectors and Trunk Beam Clusters

2.1.1 Optics Design

In microwave optics the standard dual reflector system, derived from the Cassegrain optical telescope, utilizes a parabolic main reflector and a smaller hyperbolic subreflector and is known to provide a rather wide scan angle without excessive beam distortion. This Cassegrain antenna was investigated for the present application, and it was found that the optimum arrangement could not provide the required scan angle of 3.2 degrees off-axis.

An earlier FACC investigation of the Schwarzschild dual reflector antenna, which has a much larger subreflector, had shown that this design offers promise for wide angle scanning. The Schwarzschild design was therefore investigated for this MBA application. The conclusion reached was that the design could be made suitable provided the feed array aperture was a double curved surface.

Since it appeared that there were a number of new problems in building a waveguide network to feed a curved aperture array, it was decided to investigate the use of more general reflector surfaces that would work with a flat feed aperture.

The Cassegrain and Schwarzschild antennas each have reflectors that are partial surfaces of revolution about an axis. Fabrication of the reflectors (or molds for use in forming these reflectors) can be done by rotating a fixed curve template about the axis of symmetry to cut material away until the desired final surface is reached. This feature clearly can be a great convenience during manufacture. Removing this symmetry feature provides additional degrees of freedom that may permit better electromagnetic performance, but this gain is at the expense of more complex manufacture. Nevertheless, it was felt that it was preferable to give up reflector axial symmetry rather than use a curved feed aperture surface.

The definition of more suitable main and subreflector surfaces was accomplished by use of ray tracing procedures to select the most appropriate surfaces for minimizing path length variation for beams that cover the required area. The actual procedure is as follows:

- Select an appropriate Cassegrain reflector feed system that provides the required coverage of 3.0 x 6.4 degrees.
- Compute pathlength variations for beams that cover the defined area.
- Modify both reflector surfaces and recompute pathlength variations.
- Iterate until the mean pathlength variation is minimized.
- Compute typical beam patterns; Repeat above as required.

In all cases the large main reflector was efficiently illuminated, that is, it was not oversize. To maintain this illumination the subreflector was oversize. In fact this large subreflector is the key to the good performance in this free form reflector system just as it is for the Schwarzschild antenna system. The primary beam illumination spot on the subreflector moves about the surface as the beam is shifted in position.

By following the above iterative process with some trade-offs of basic dimensions a final design, C41.2, shown in Figure 2.5 was developed. This design has a pathlength variation of less than 0.1 wavelength for the entire rectangular scan area. It is interesting to note that this antenna design does not have any focal point where there is zero pathlength error. In fact the pathlength error for the central beam is about the same as for any other beam.

Confirmation of the quality of this reflector design was achieved by calculating on-and off-axis single beam radiation patterns for the CONUS field of view. The exceptional quality is displayed in Figures 2.6 and 2.7 where it can be noted that the scan gain loss is less than 0.4 dB and the first sidelobes change by only 2.0dB.

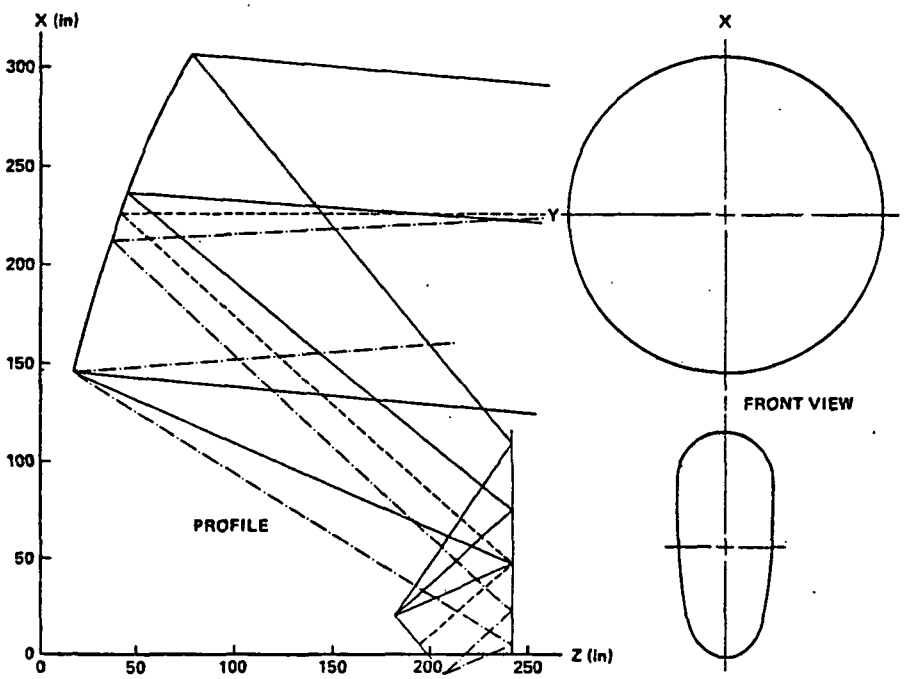

Figure 2.5 NASA 30/20 GHz Reflectors and Feed Configuration

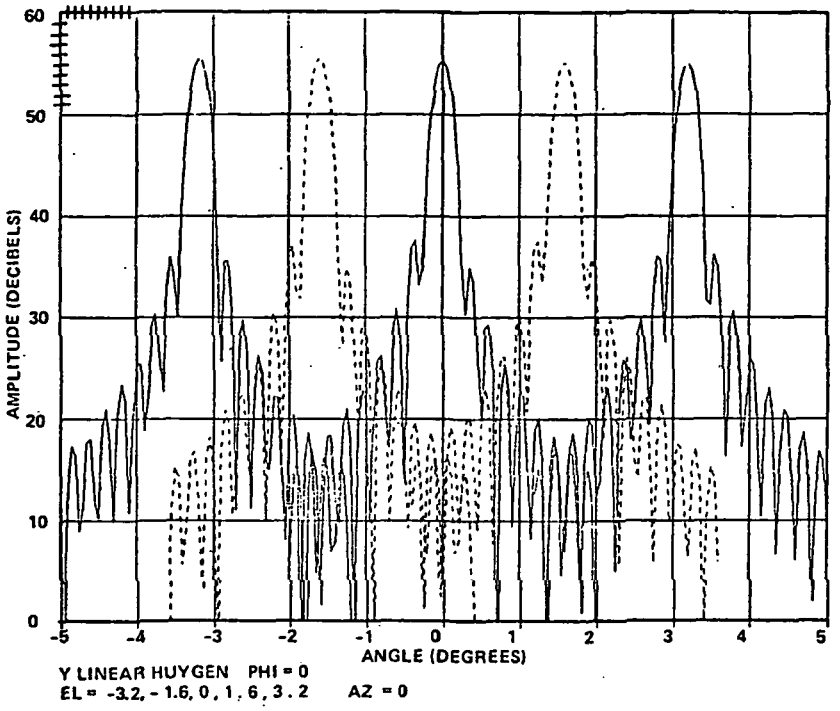

Figure 2.6 Calculated Patterns of Consituent Beams of Design C41.2

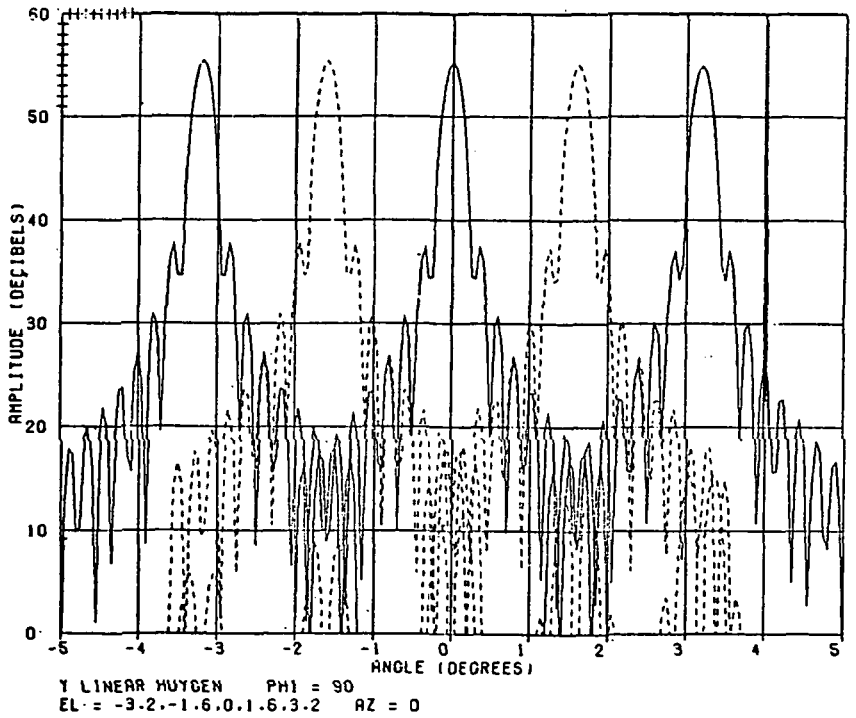

Figure 2.7 Calculated Patterns of Constituent Beams of Design C41.2 (continued)

2.1.2 Beamforming Network and Array Design

The CONUS feed array configuration for the dual reflector design, C41.2, is shown in Figure 2.4. The element aperture is two wavelenths square. The normal 7-element cluster selected for both scan and trunk beams provides suitable low sidelobes with little gain reduction from the ideal value over the entire CONUS region. If required for a particular region, the number of cluster elements for a trunk beam can be increased to 13 or some other higher value.

As indicated in Figure 2.4 the scan coverage is accomplished in 6 independent scan sectors with a maximum of 102 horns in a sector. A beamforming network (BFN) for each sector consists of an 8 to 1 power division tree, eight phase shifters and eight 16 to 1 switch matrices as shown in Figures 2.8 and 2.9. This BFN permits the selection of any one 7-element cluster by use of the switch matrix. The variable power dividers and variable phase shifters are used to set the amplitude and phase for each active horn. The active network elements are ferrite devices, described later, that make rapid beam switching a reality.

A pictorial drawing of the complete waveguide BFN for one of the 6 sectors is displayed in Figure 2.10. This drawing includes orthomode junctions (OMJ's) for connecting in the other polarization wherever that is required.

The trunk coverage is accomplished by connecting the appropriate feed horns to the trunk lines by use of frequency diplexers and/or orthomode junctions as illustrated in Figure 2.8.

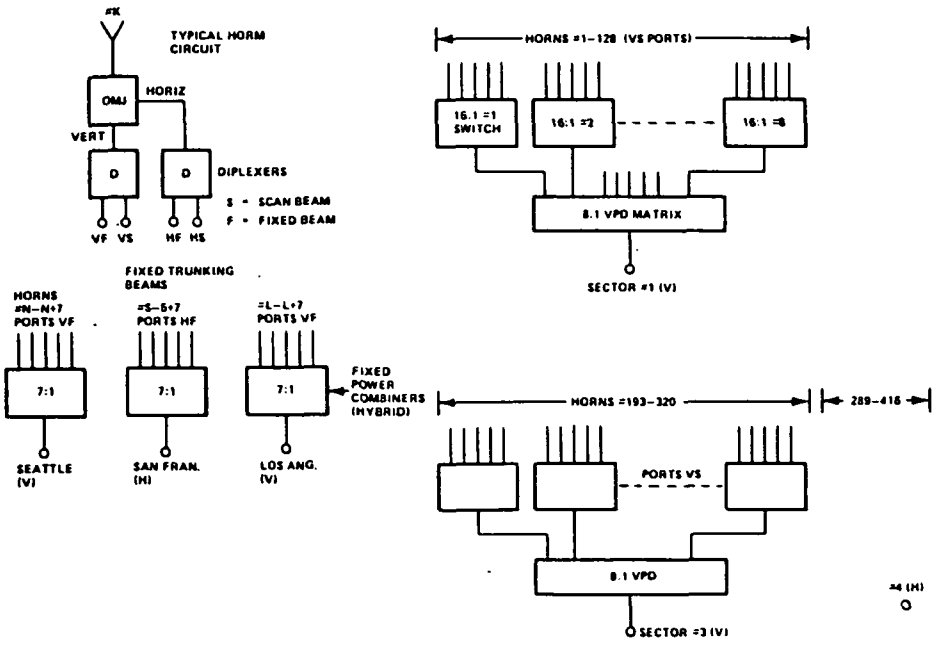

Figure 2.8 Beamforming Network for Operational Satellite

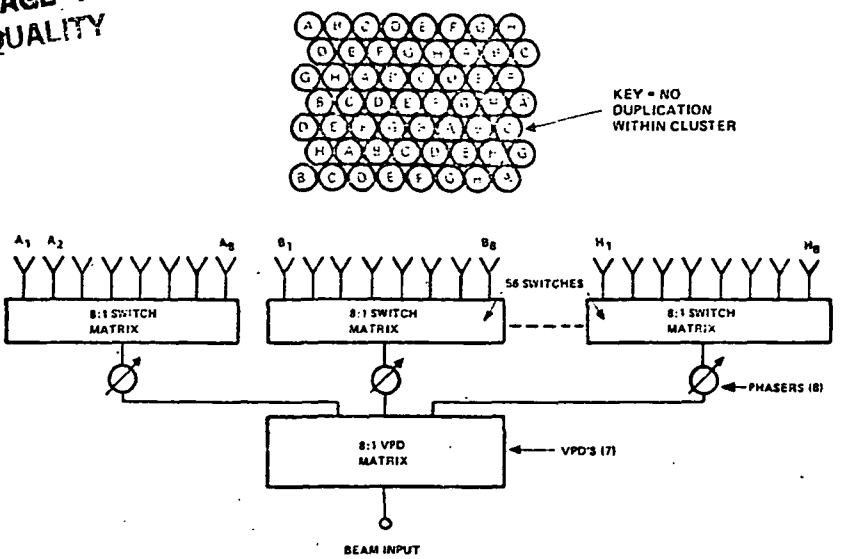

Figure 2.9 Scan Beamforming Network

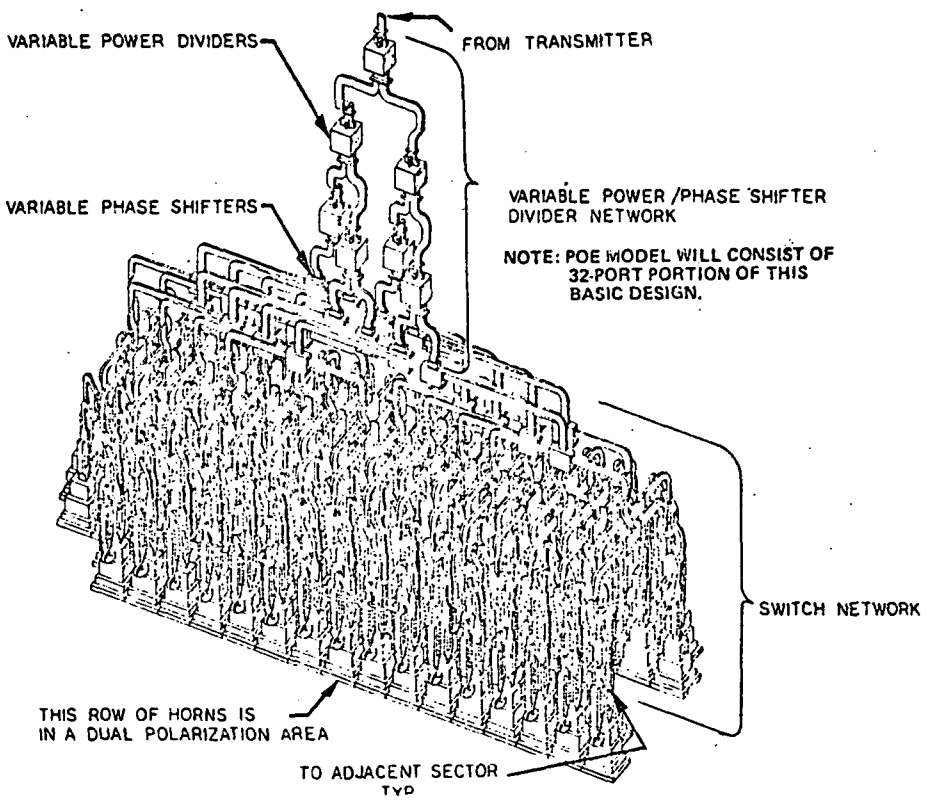

Figure 2.10 128-Port Scan Beamforming Network

2.2 Demonstration Concept

During the course of developing a concept for the SOW's demonstration system it was found that a less complex system could provide all the desired features. So this new system was recommended and accepted. The new demonstration MBA is identical to the Operational MBA except for the feed array which is

Table 2.1 Demonstration Satellite MBA System Weight and Stowed Volume (Noncompliant)

COMPONENT	DOWNLINK		UPLINK	
	Mass (Pounds)	Stowed Volume (cu. ft.)	Mass (Pounds)	Stowed Volume (cu. ft.)
Main Reflector	73.0		24.0	
Subreflector	11.5	228	5.0	72
Support Structure	15.7		7.3	
Subtotal	100.2		36.3	
Feed Array	5.9		3.6	
Diplexers	9.0		5.4	
OMJ's	29.0		17.4	
Waveguide	3.1	1.5	1.9	1.5
Elbows, Flanges, etc	5.9		3.6	
VPD, VPS, Switches *	17.9		10.8	
Support Plates	10.7		10.7	
Subtotal	81.5		53.4	
Deployment Mechanism	8.8		8.8	
	227.5		73.5	

* With Drivers

considerably simplified to scan only two sectors and provide only eight trunk beams as illustrated in Figures 2.11 and 2.12. Flight testing of this system could prove out all of the operational MBA features. Preliminary weights and volumes for the demonstration satellite MBA's are given in Table 2.1

2.3 Proof-of-Concept Model Specification

A Laboratory model to provide proof-of-concept consists of a 30 GHz MBA with a simplified feed array and BFN. Both the scan and trunk arrays are small and movable over the entire operational array area so that any operational beam can be generated and its characteristics measured. These arrays and BFN's are large enough to include all of the operational features of these units. The key features of the POC model are listed in Table 2.2 and the design and fabrication is described in Section 4.

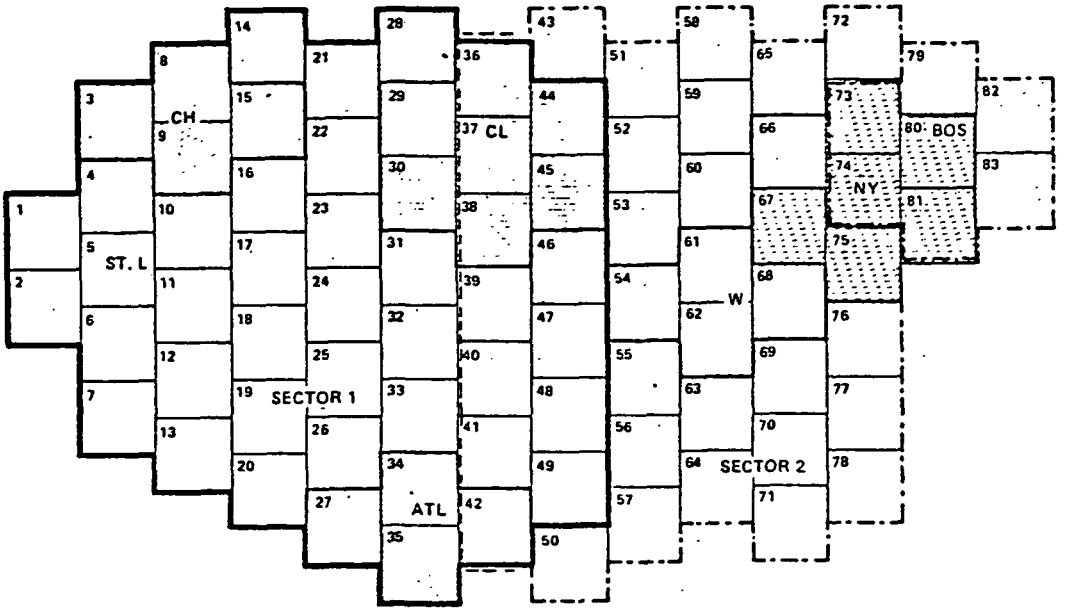

Figure 2.11 Feed Horn Layout for Recommended Demonstration Satellite

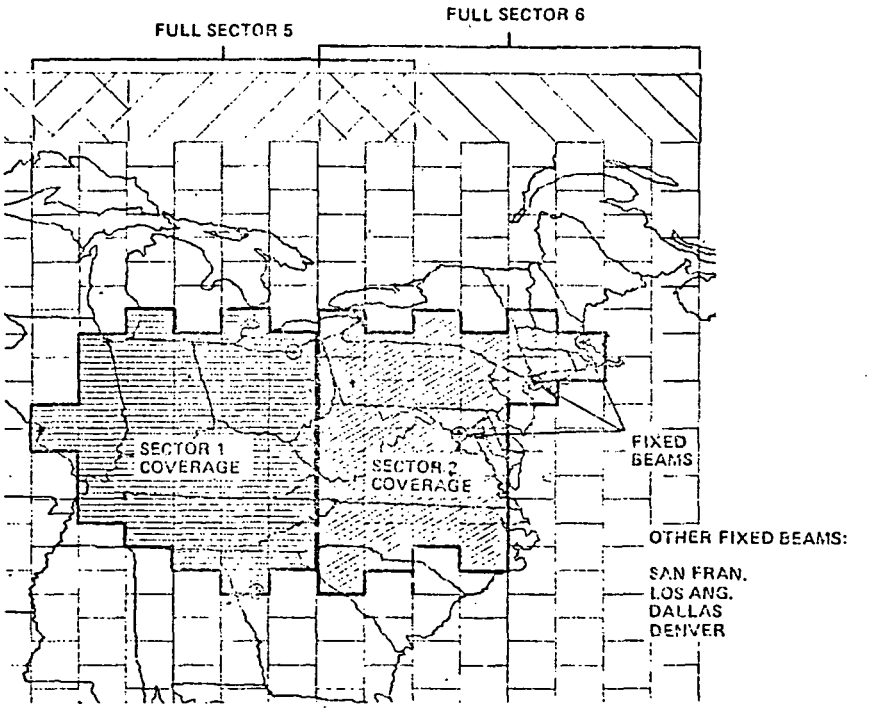

Figure 2.12 Recommended Demonstration Satellite Coverage

TABLE 2.2

POC MODEL DESIGN SUMMARY

- o Optics
  - Aluminum offset dual shaped reflectors 13.5 ft aperture diameter, 0.3^{o} BW
- o Feed array
  - Trunk cluster of 13 copper horns with OMJ's
  - Partial CPS scan sector of 54 copper horns
  - Feed positioning mechanism of steel
- o BFN
  - Trunk 1 to 13 port divider of copper with mechanically adjustable coefficients
  - CPS 1 to 32 port electronically scannable BFN of copper with ferrite switches, VPS's and VPD's
- o CPS beam controller
  - Allows adjustment of ferrite elements for any beam position with controlled amplitudes and phases to 7-element cluster.
- o Structural tower
  - Steel tubular welded structure

3.0 Component Development

All non-commercial components for the POC Model were built and tested in breadboard form. The specialized ferrite switching and control components used in the scan beam network were developed at Electromagnetic Sciences, Inc. in Atlanta, Georgia, and the remaining passive waveguide components were developed at FACC in Palo Alto, California.

Desired specifications were defined for each component, and after fabrication, measurements were made on each to determine deviations from specification.

Layouts of the scan and trunk beam systems, showing application of many of the key componets, are given in Section 4. In addition to those shown, there are a number of passive waveguide components. The remaining parts of this section summarize the breadboard components' design.

3.1 Scan Beam Components

The scan beam network consists of a combination of variable phase shifters (VPS's),variable power dividers (VPD's), circulator switches and interconnecting waveguide sections. Design and manufacture of the waveguide sections were rather complex because of the necessity for keeping all input-output paths of equal length to provide the required wide bandwidth.

3.1.1 Variable Power Divider

The VPD shown in Figure 3.1 is a dual toroid ferrite device that employs two 90 degree phase shifters between waveguide couplers. The input coupler is a folded hybrid tee using the sum port as the input, and the two outputs mate to the phase shifter inputs. The outputs of the phase shifters drive two ports of a waveguide short slot coupler and the remaining two ports of the coupler form the output ports of the VPD. By proper selection of the two phase shifter settings, the power from the input port (split by the magic tee) can be routed to either of the outputs in any power division ratio, ranging from all power to one VPD output port or all power to the other port. Figure 3.2 is a photograph of the actual device and its associated driver.

3.1.2 Variable phase shifter

The VPS is a dual toroid ferrite device in WR42 rectangular waveguide. The configuration shown in Figure 3.3 has a dielectric layer separating the two toroids. A photograph of the device is shown in Figure 3.4

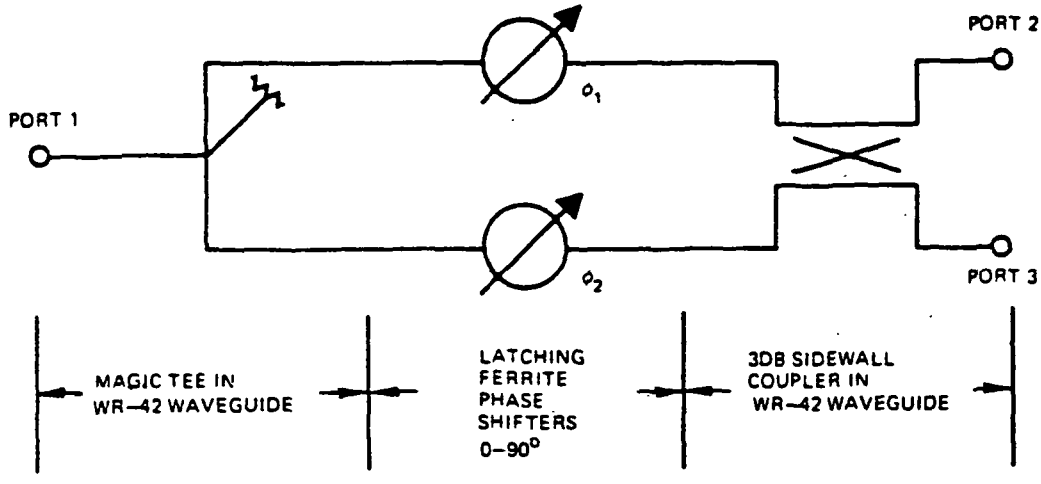

Figure 3.1 VPD Layout

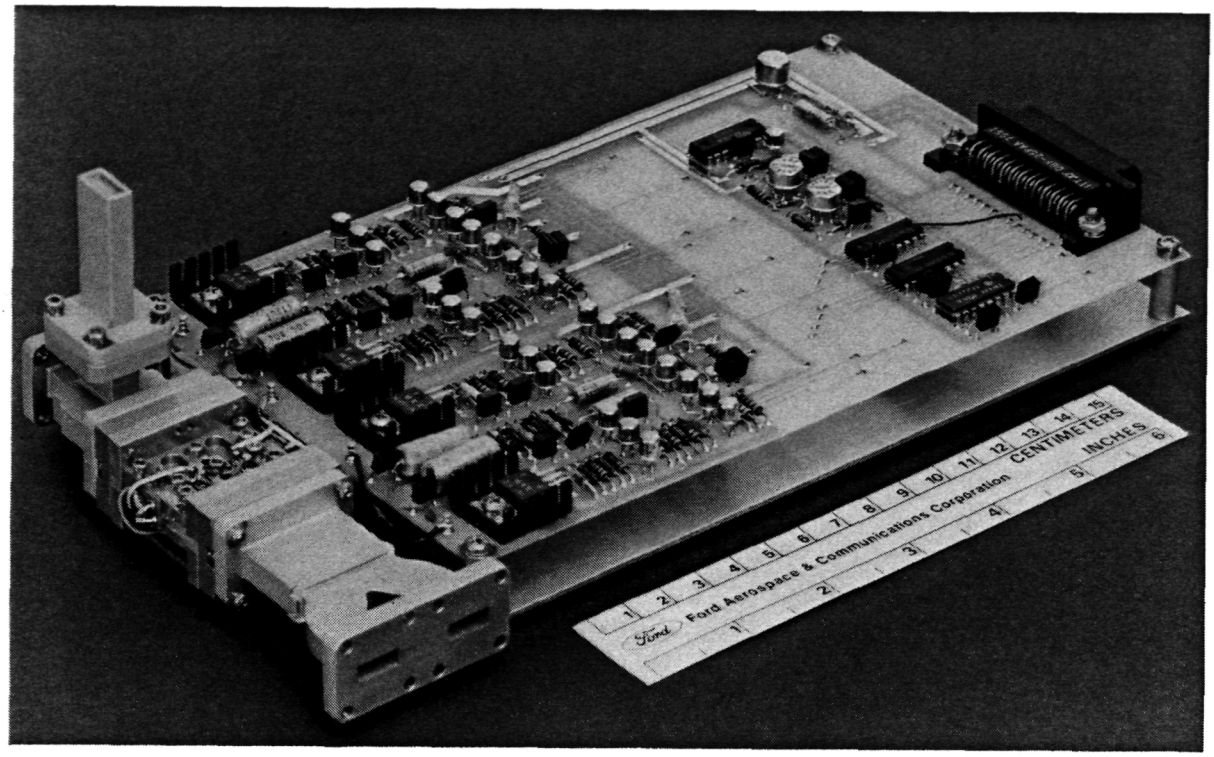

Figure 3.2 Breadboard VPD and Driver

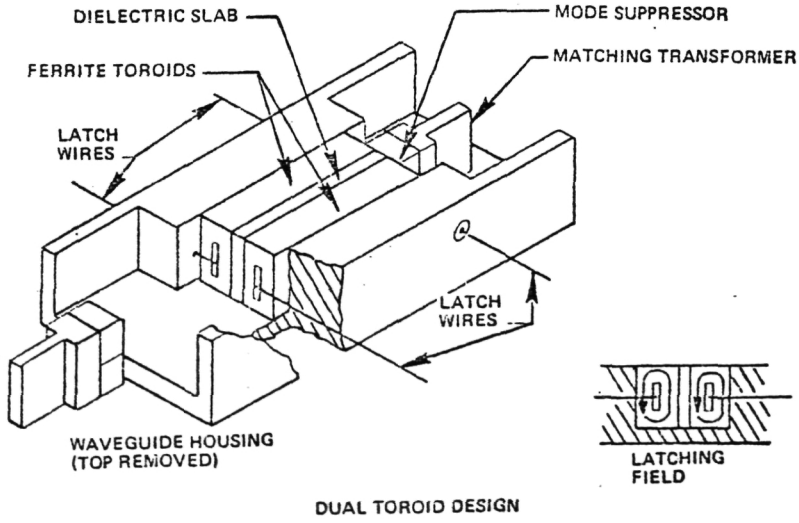

Figure 3.3 VPS Layout

3.1.3 Switching Circulator

The switching circulator is a three-port ferrite device with a triangular cross-section ferrite piece symmetrically positioned at the junction of the three ports. It is used as a very fast electrically operated switch. A pictorial drawing of the unit appears in Figure 3.5 and a photograph is shown in Figure 3.6.

3.1.4 Ferrite Component Summary

The design goals and the performance predicted from measurements on the breadboard components are given in Figure 3.1. It appears that all of the goals have been met.

3.2 Trunk Beam Components

The components for the trunk beam network include a variety of fixed power dividers and waveguide connecting lines as illustrates in Figure 3.7. All components were fabricated in copper. These devices with their measured performance are listed in Table 3.1.

3.3 Common Array Components

The components common to both the scan and trunk systems include horn radiators, orthomode junctions (OMJ's) and diplexers. These met all the specified goals when tested as shown in Table 3.2.

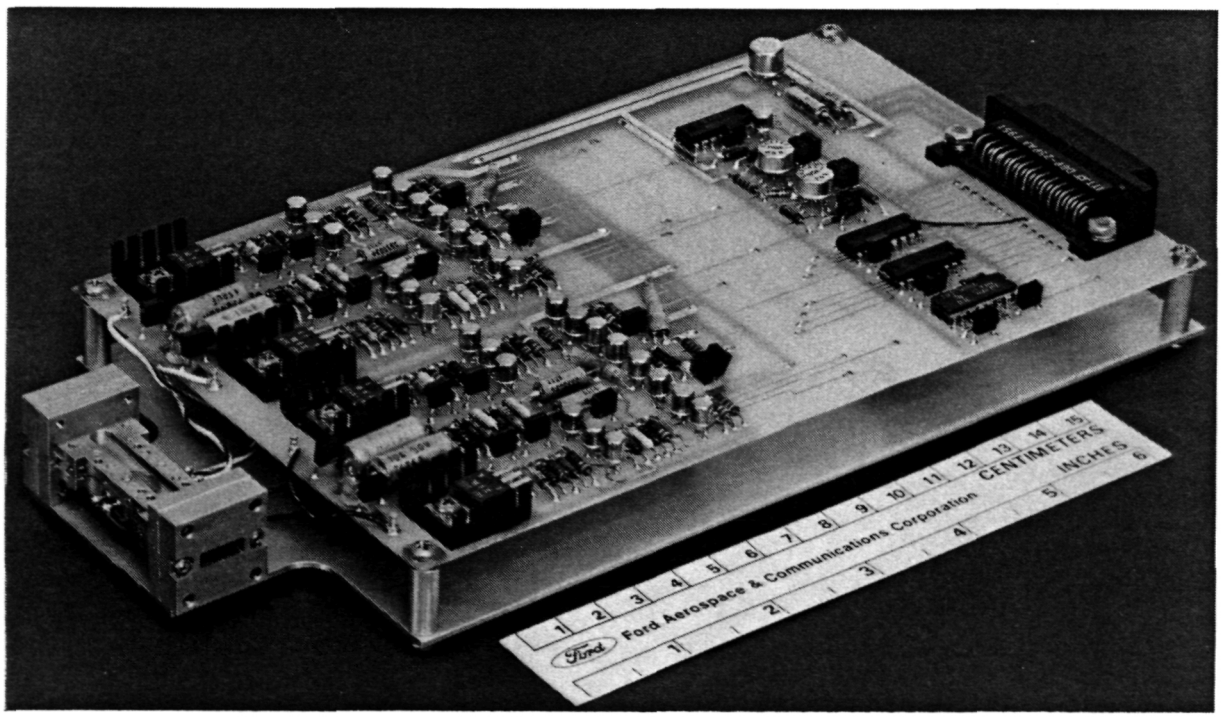

Figure 3.4 Breadboard VPS and Driver

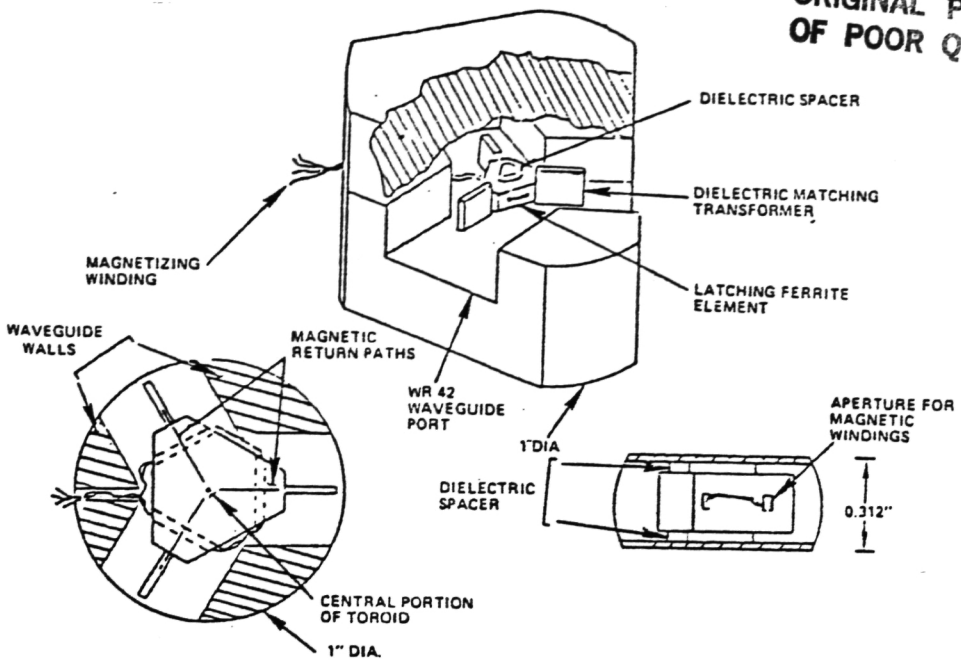

Figure 3.5 Switching Circulator Layout

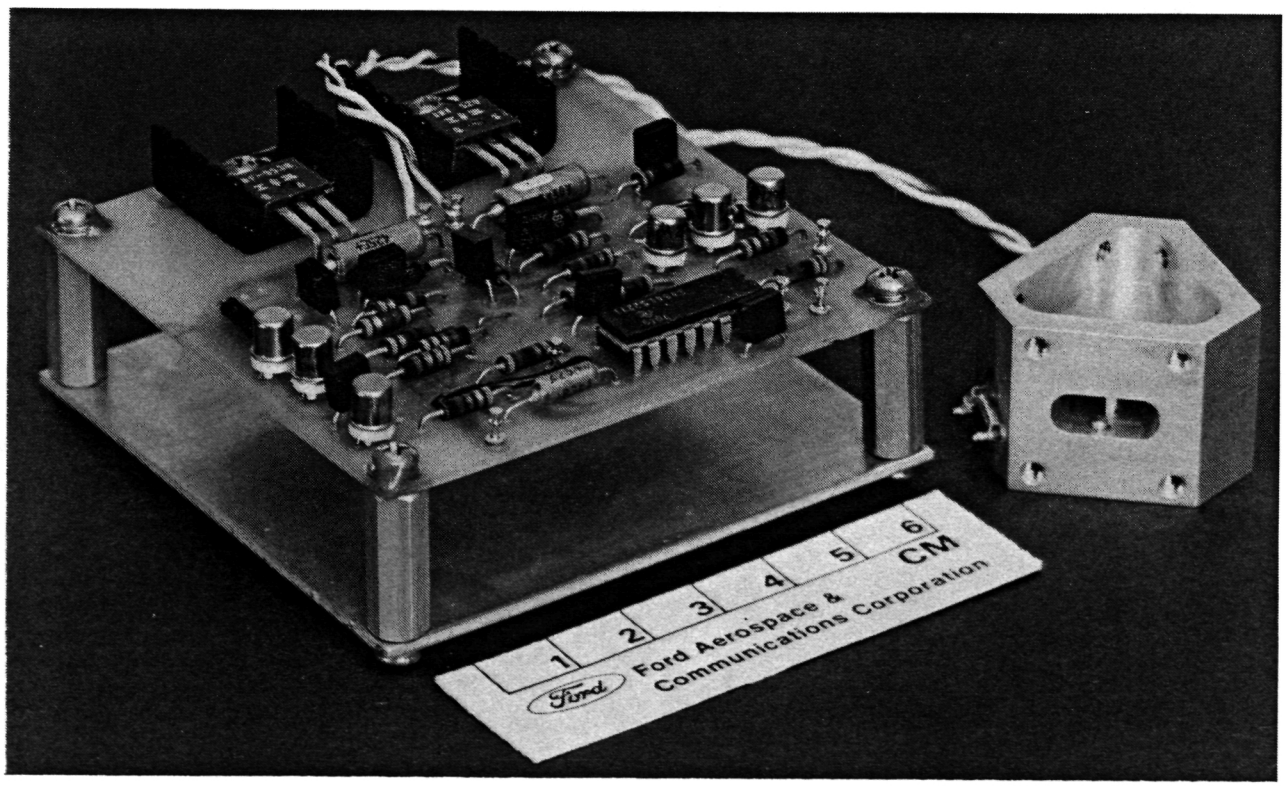

Figure 3.6 Breadboard Switching Circulator

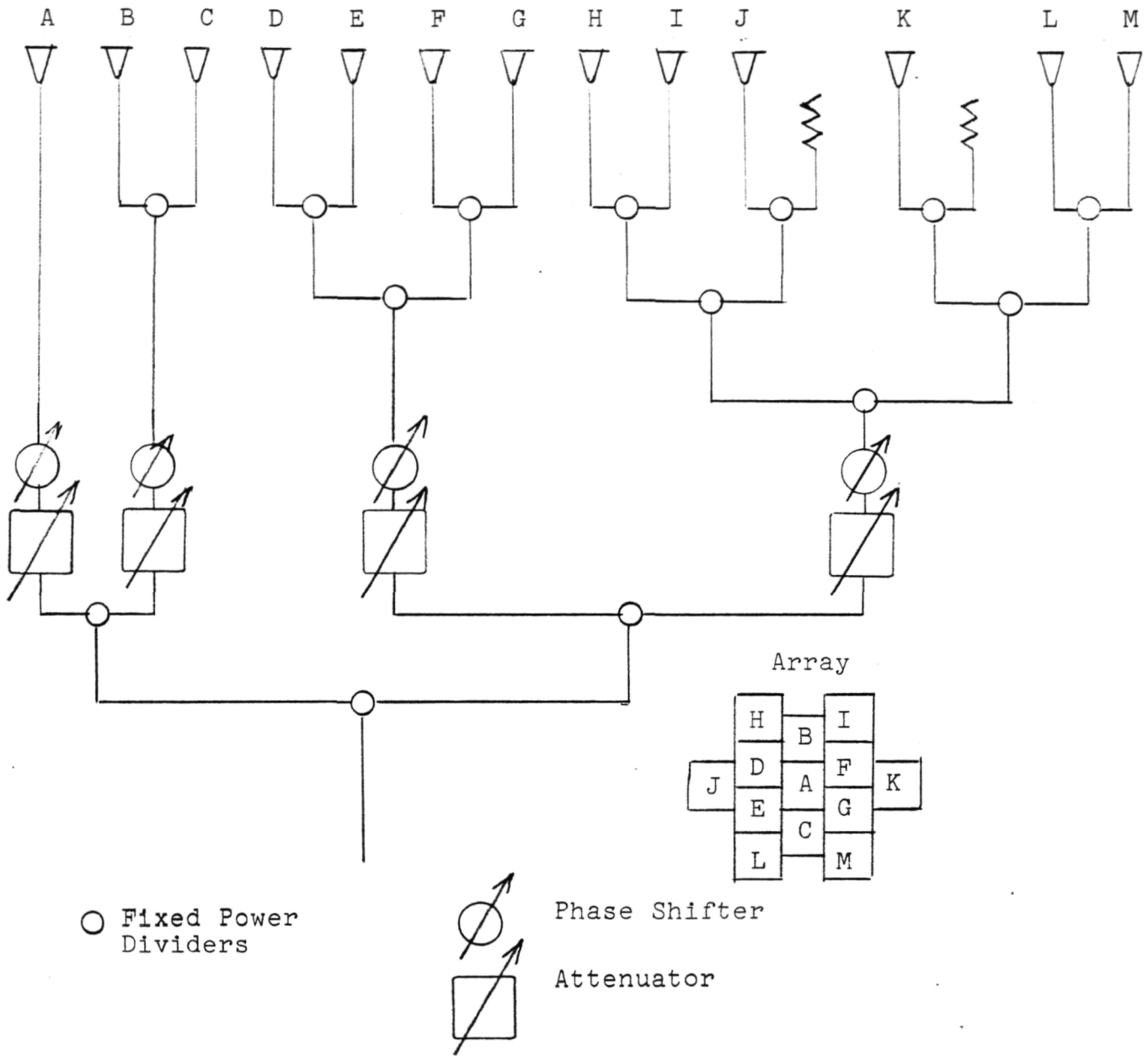

Figure 3.7 Fixed Beam Network Layout

Table 3.1 Scan Beam System and Common Component Performance Summary

VARIABLE POWER DIVIDER (LATCHING, NONRECIPROCAL)

Parameter	Design Goal	Predicted Performance
Frequency range (GHz)	18.85-19.35	18.85-19.35
Power ratio range dB	0 to ±20	0 to ±20
Insertion loss, dB any setting	0.6	0.5*
VSWR, max	1.2:1	1.2:1*
Output-to-output isolation, dB	20	20*
Phase shift/power division accuracy	Per table	Per table
Size (excluding drivers) max	1.25 x 0.75 x 3.0 inches	1.25 x 0.75 x 3.3 inches
Weight (excluding drivers) max	TBD	1.8 oz
Power handling, Watts CW	60	60
Switching energy, μj max**	300	75*
Switching rate, max	25,000 Hz	25,000 Hz
Temperature range (°C)	0 - 50°	0 - 50°

VARIABLE PHASE SHIFTER (LATCHING, NONRECIPROCAL)

Parameter	Design Goal	Predicted Performance
Frequency range (GHz)	18.85-19.35	18.85-19.35
Phase shift range dB	0 - 360°	0 - 360°
Insertion loss, dB max	0.8	0.7
VSWR, max	1.2:1	1.2:1*
Phase accuracy	±°	±°
Number of bits	6	6
Switching time, max	0.5 μsec	0.4 μsec*
Switching energy, μj max**	300	75*
Switching rate	25,000 Hz	25,000 Hz
Phase variation (over temp & freq)	10°	10°
Size (excluding drivers) max	1.25 x 0.75 x 3.0 inches	0.75 x 0.75 x 2.0 inches
Power handling, Watts CW	40	40
Temperature range (°C)	0-50°	0-50°

SWITCHING CIRCULATOR (LATCHING)

Parameter	Design Goal	Predicted Performance
Frequency range (GHz)	18.85-19.35	18.85-19.35
Insertion loss, dB	0.3	0.15*
Isolation to third port	23 dB	23 dB*
VSWR	1.15:1	1.15:1*
Shape	Triangular X-sect	Triangular X-sect
Size (excluding driver, max)	1 in/face x 0.312 in hi	1 in/face x 0.312 in hi
Weight (excluding driver)	TBD	0.42 oz
Switching energy, μj max**	150	40*
Switching time (μsec)	0.5 μsec	0.4 μsec*
Switching rate (max)	25,000 Hz	25,000 Hz
Power handling, Watts CW	30	30
Temperature range (°C)	0 - 50°	0 - 50°

*Measure values
**Includes losses in drivers

Table 3.2 Trunk and Scan Beam System Component Performance Summary

Component	Parameter	Design Goal	Measured Performance	POC Recommendation
Short slot coupler 1:1 power division	• Insertion loss • VSWR • Isolation • Amplitude response	0.25 dB 1.2 20 dB Flat	0.20 dB 1.06 21 dB Flat	Satisfactory
Short slot coupler 2:1 power division	• Insertion loss • VSWR • Isolation • Amplitude response • Weight	0.25 dB 1.2 20 dB Flat Min	0.19 dB 1.2 20 dB Flat 28.4 grams	Satisfactory
Branchguide coupler 5:1 power division	• Insertion loss • VSWR • Isolation • Amplitude response	0.25 dB 1.2 20 dB Flat	0.18 dB 1.15 20 dB Flat	Satisfactory, exact power division is off 0.25 dB, but could be corrected
Branchguide coupler 10:1 power division	• Insertion loss • VSWR • Isolation • Amplitude response	0.25 dB 1.2 20 dB Flat	0.15 dB 1.09 25 dB Flat	Satisfactory, exact power division is off 0.25 dB, but could be corrected
Branchguide coupler 3:1 power division	• Insertion loss • VSWR • Isolation	0.25 dB 1.2 20 dB	0.1 dB 1.05 18 dB	Poor isolation due to bent WG at input
Three-way power divider	• Insertion loss • VSWR • Amplitude ratio	Min 1.1 Equal	~ 0.1 dB 1.05 Equal	Satisfactory
Flangeless Interconnect	• Insertion loss • VSWR	0.05 1.1	0.03 dB 1.07	Satisfactory
Feed horn	• VSWR • Principal pol. • X-pol level • Weight	1.2 Unimode -35 dB Min	1.15 Unimode -35.7 dB 23.3 grams	Satisfactory
Horn/OMJ	• VSWR • Coupling level • X-pol Contribution	1.2 -35 dB -35 dB	1.17 -35 dB -36.1 dB	Satisfactory
Diplexer	• Passband VSWR • Stop band rejection • Insertion loss	1.2 15 dB 0.5 dB	1.15 16 dB 0.6 dB	• Must retune to achieve exact band placement • Loss could be improved to 0.5 dB

4.0 POC Model Design and Fabrication

As mentioned in Section 2.3 the proof of concept model makes use of the operational reflectors but uses small movable feed arrays to excite the desired beams. The model consists of the following key components:

Main reflector	Theodolite platform
Subreflector	Dynamic alignment monitors
Support structure	Standard gain antenna
Feed array and network	Reference antenna
Feedrack	Pedestal
Cover box for feed	Control wiring

The reflectors have optimized shaped reflectors and are fabricated from aluminum. These reflectors and the feedrack are supported by a tubular steel structure mounted on a large Scientific-Atlanta pedestal. The steel feedrack that supports the feed array is designed to allow precise positioning of the array anywhere within the defined X-Y plane. The drawing of Figure 4.1 displays the relative positions of the key components installed on the range tower. As indicated in the drawing counter weights are attached to balance the MBA unit about the central boresight axis and about the elevation axis. Features of the POC model components are described in the remainder of this section.

4.1 Reflectors

As previously mentioned both reflectors have shaped surfaces that have no axial symmetry and these surfaces must therefore by formed or machined point by point. In addition to being accurately formed the surface should have minimum deflection from gravity loading. Otherwise the quality of the beams will deteriorate. The basic manufacturing surface tolerance specification was:

- Systematic error - 0.015 inch
- Random error - 0.003 inch
- Finish - 32 microinch

where these maximum errors were to be maintained for the reflectors placed in any attitude on the test range.

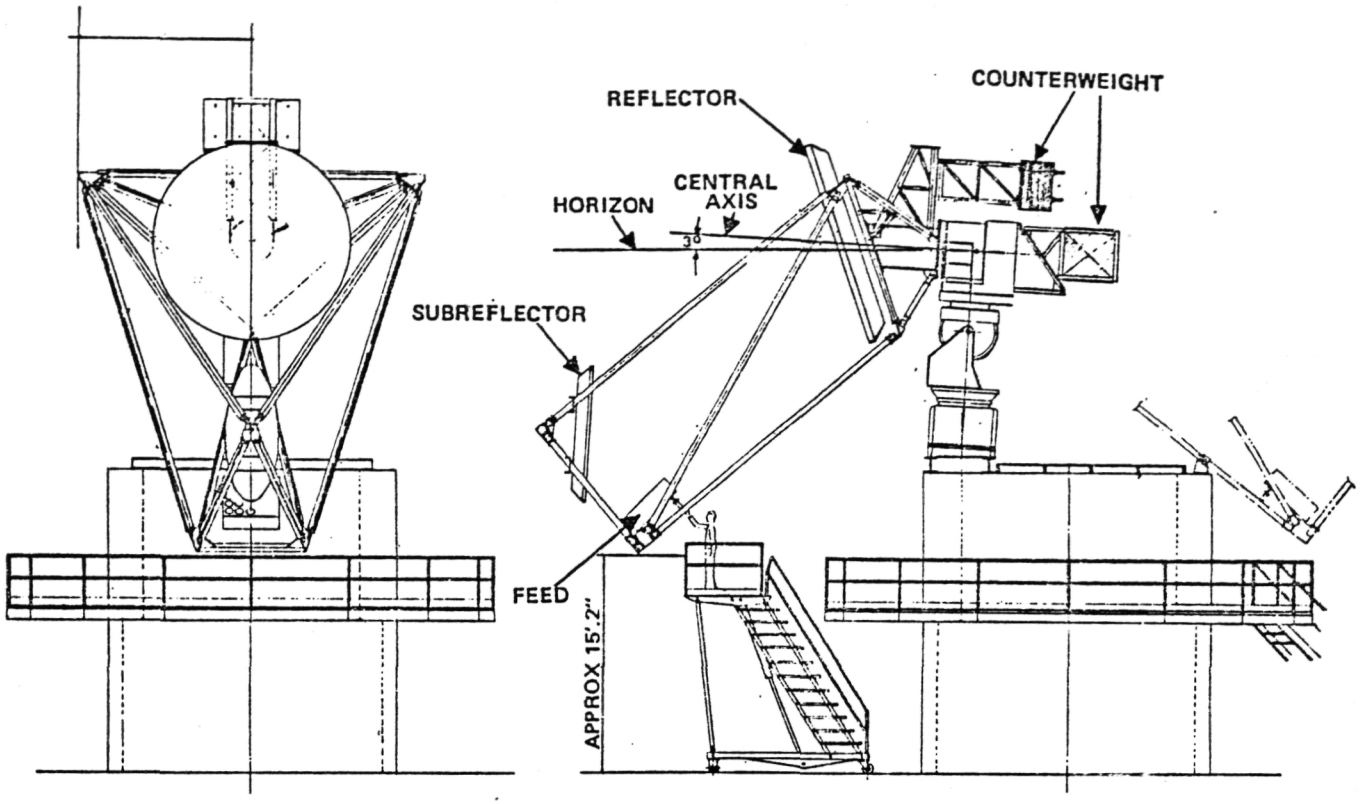

Figure 4.1 POC Model MBA

To minimize cost NASA approved the use of aluminum, rather than flight type material such a graphite epoxy for the fabrication. The mechanical design makes use of truss supported triangular plates, bolted and cemented together as shown in Figure 4.2. The final surface forming is done by machining on a large horizontal shaft contouring engine.

Before surface machining the narrow (less than 1/8 inch) groove between adjacent plates was filled with an epoxy material containing aluminum powder. After final machining the groove lines were coated with a conducting silver paint and the entire surface was then painted white.

The measured variations from surface specification showed that both reflectors were well within the required tolerance. (See the contour plot for the main reflector in Figure 4.3).

The reflectors' structural design, fabrication, and surface machining were all done by Tinsley Laboratories in Berkeley, California.

4.2 Support Structure and Feedrack

The tubular steel support structure, counter weight frames, and feedrack, illustrated in Figures 4.4 and 4.5, were designed to support the reflectors and arrays without intoducing mechanical strains into these units or interfering in any way with the electromagnetic performance. The structure did deflect up to 0.7 inch for a 90 degree axial rotation as measured by the three lasers mounted on the reflectors for dynamic deflection monitoring.

4.3 Feed Array and Beam Forming Networks

The POC feed array aperture for forming any one of 14 electrically switched beams is shown in Figure 4.6 where the dot indicates which horns can be 7-element cluster center horns. Including the terminated dummy horns surrounding the 32 active horns, the total scan array has 56 horns. The photograph of Figure 4.5 shows the scan array mounted in the feedrack.

A schematic diagram of the beamforming network showing the horns, circulator-switches, phase shifters, and power dividers is given in Figure 4.7. Any one of the 14 clusters, can be selected and each of the 7 cluster elements can be set to any desired relative amplitude and phase value. A photograph of the Scan beamforming network and its controller is shown in Figure 4.8.

For range testing, the array polarization could be changed from horizontal to vertical by adding a short 90 degree waveguide twist section between each active horn and its waveguide feed. It was therefore unncessary to conduct range tests with the trunk feed. The trunk feed with up to 13 active elements was fabricated, however. A trunk beam network schematic diagram is given in Figure 4.9 and a photograph of the unit is in Figure 4.10

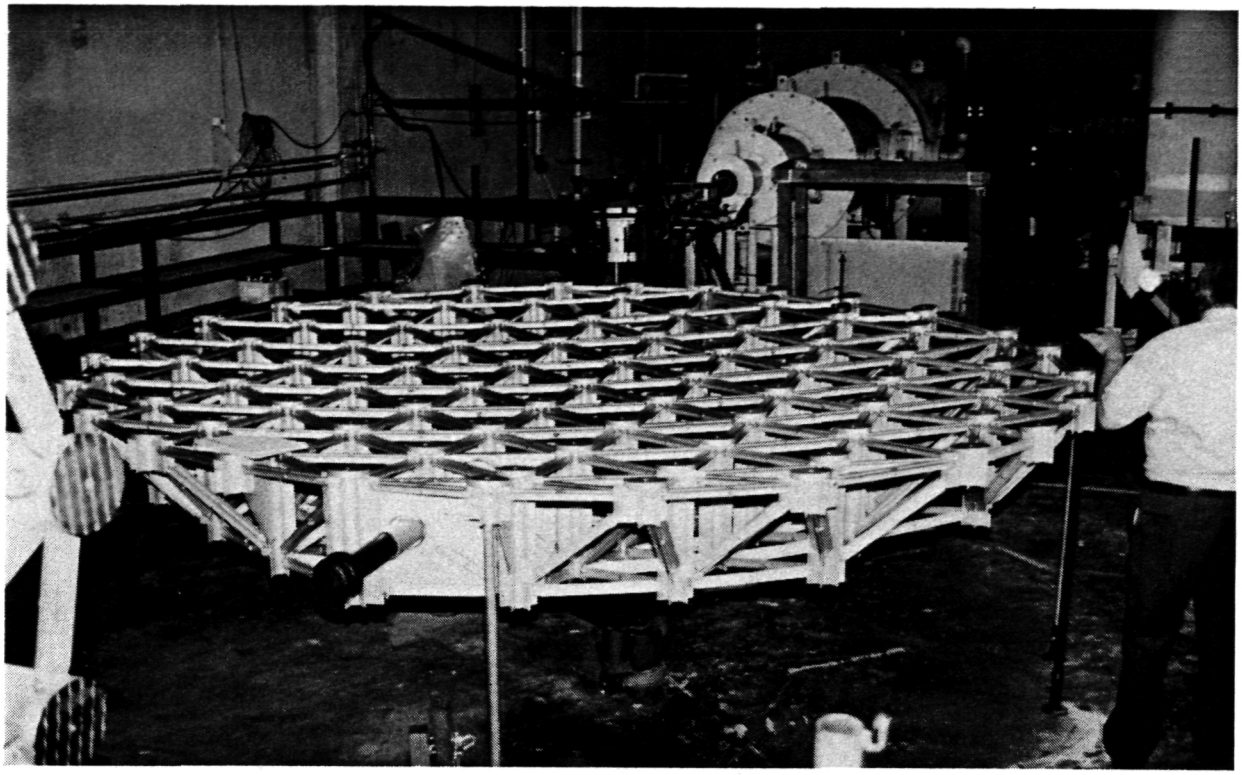

Figure 4.2 Main Reflector During Manufacture

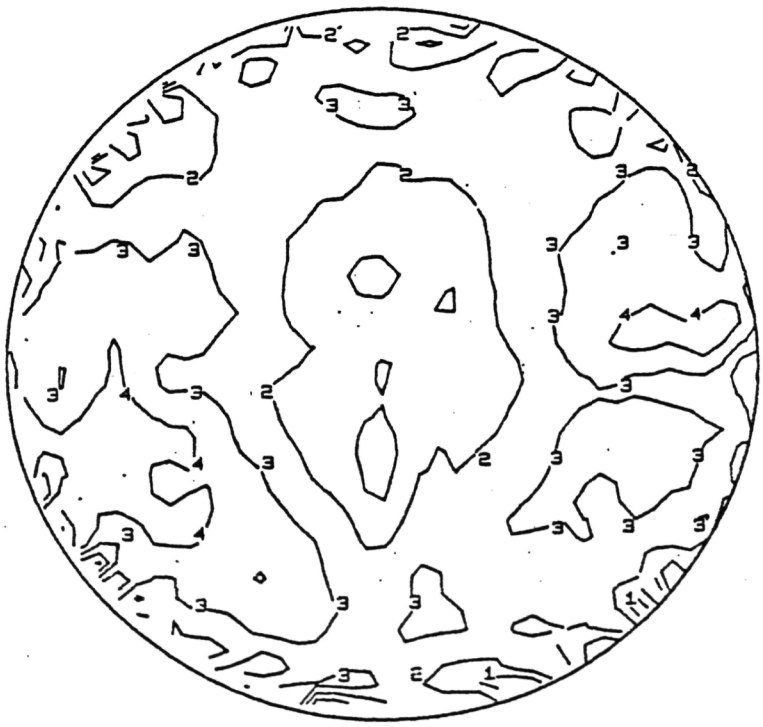

Figure 4.3 Main Reflector Surface Accuracy

CONTOUR PLOT OF FACC MAIN MEAS 2 3/23/83 54W
PEAK TO PEAK DIFFERENCE = 0.4699E-02 RMS VALUE = 0.7994E-0
SCALE = 0.4000E-01 CONTOUR INTERVAL = 0.1000E-02
TINSLEY LABORATORIES, INC MAR 25, 83

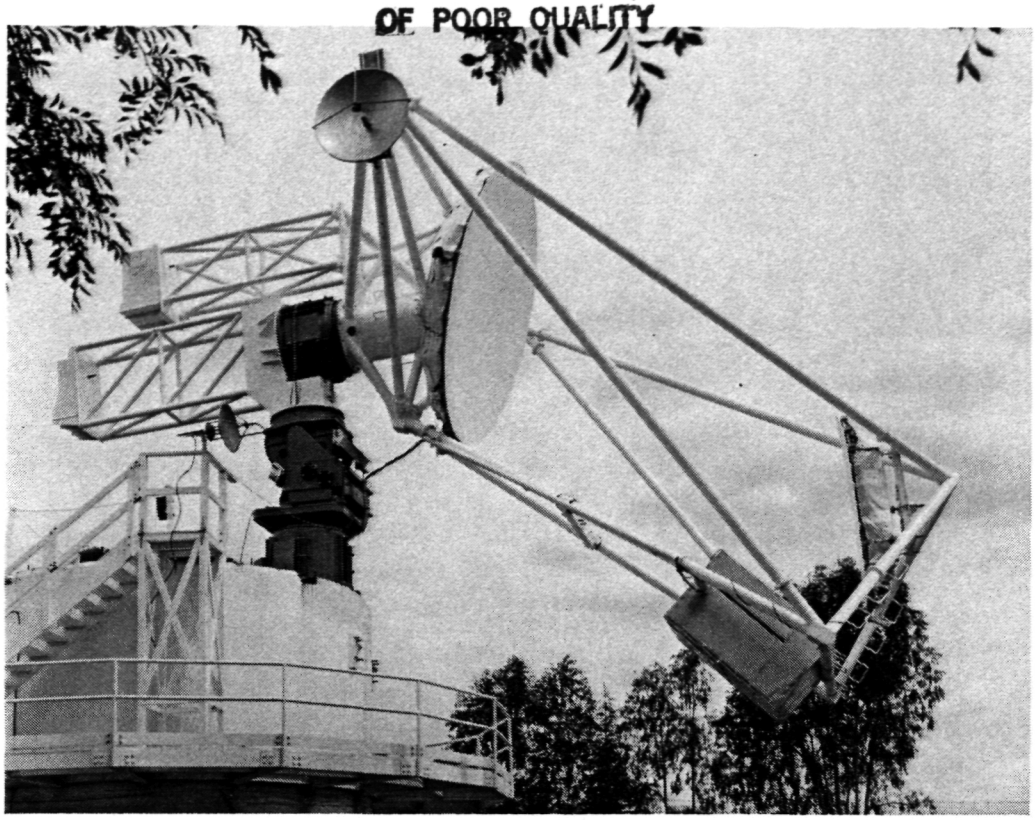

Figure 4.4 Final Assembly of NASA 30/20 GHz MBA

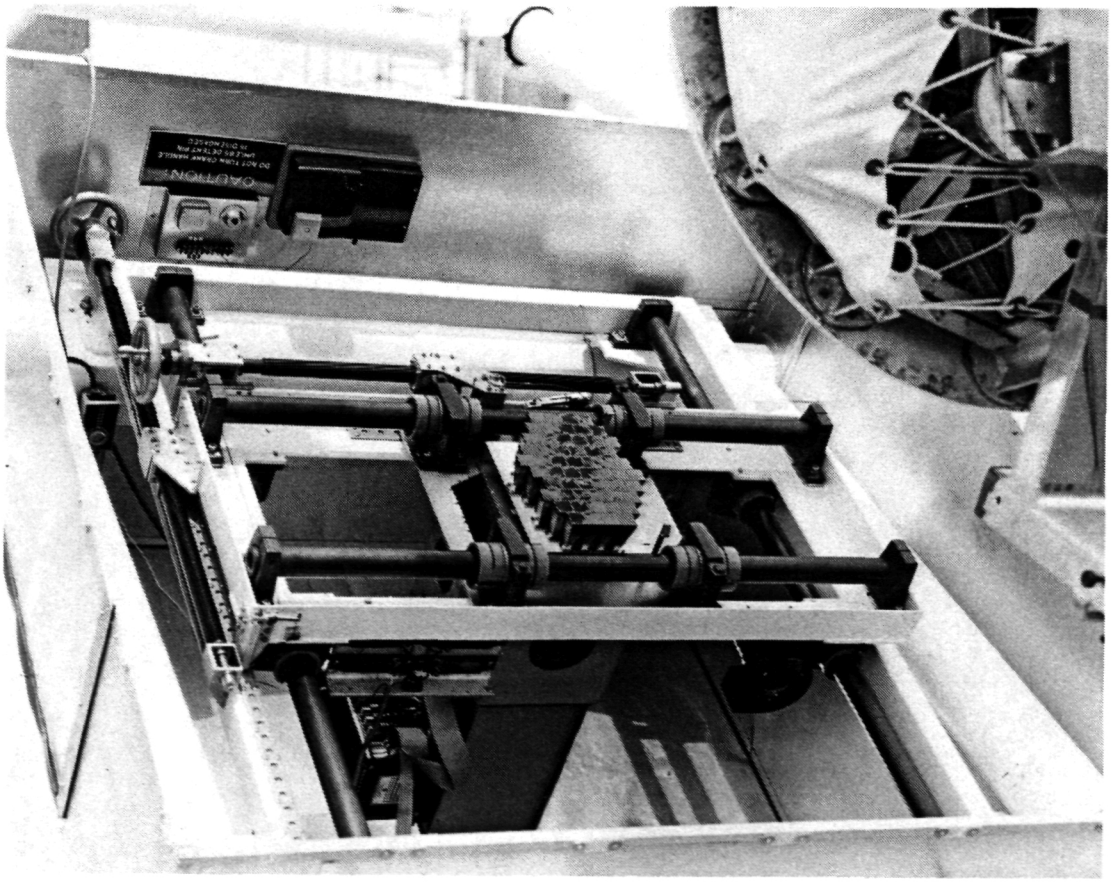

Figure 4.5 Feed Array Mounted in Feedrack

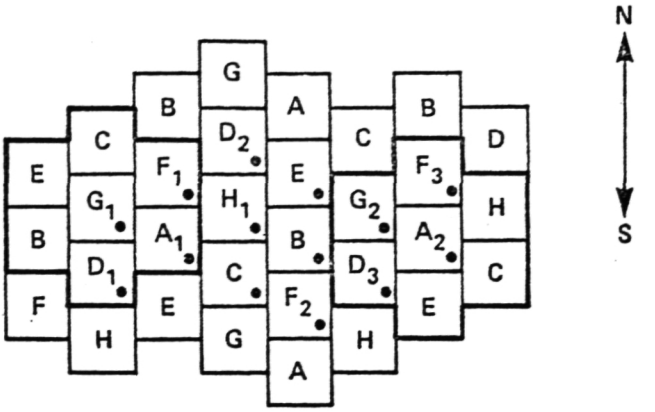

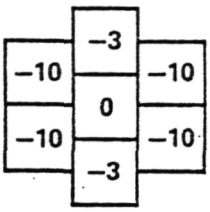

TYPICAL EXCITATION AMPLITUDES (DB)

●= POSSIBLE CENTER HORNS FOR 7-HORN CLUSTERS (14)

NOTE: ADDITIONAL ROW OF DUMMY HORNS INCLUDED AROUND ARRAYS SHOWN FOR SYMMETRY.

Figure 4.6 Scan Beam Feed Array Aperture

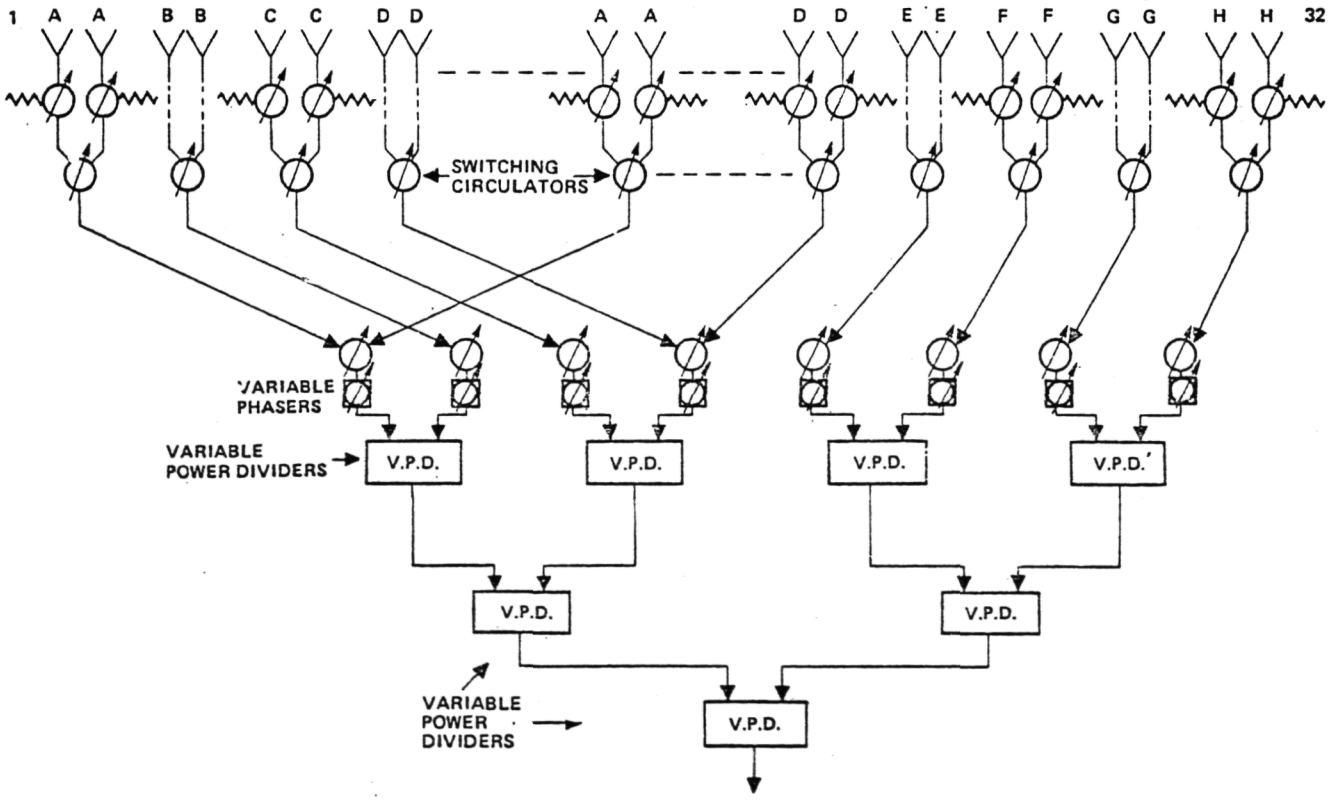

Figure 4.7 POC BFN Configuration - Scan Beam

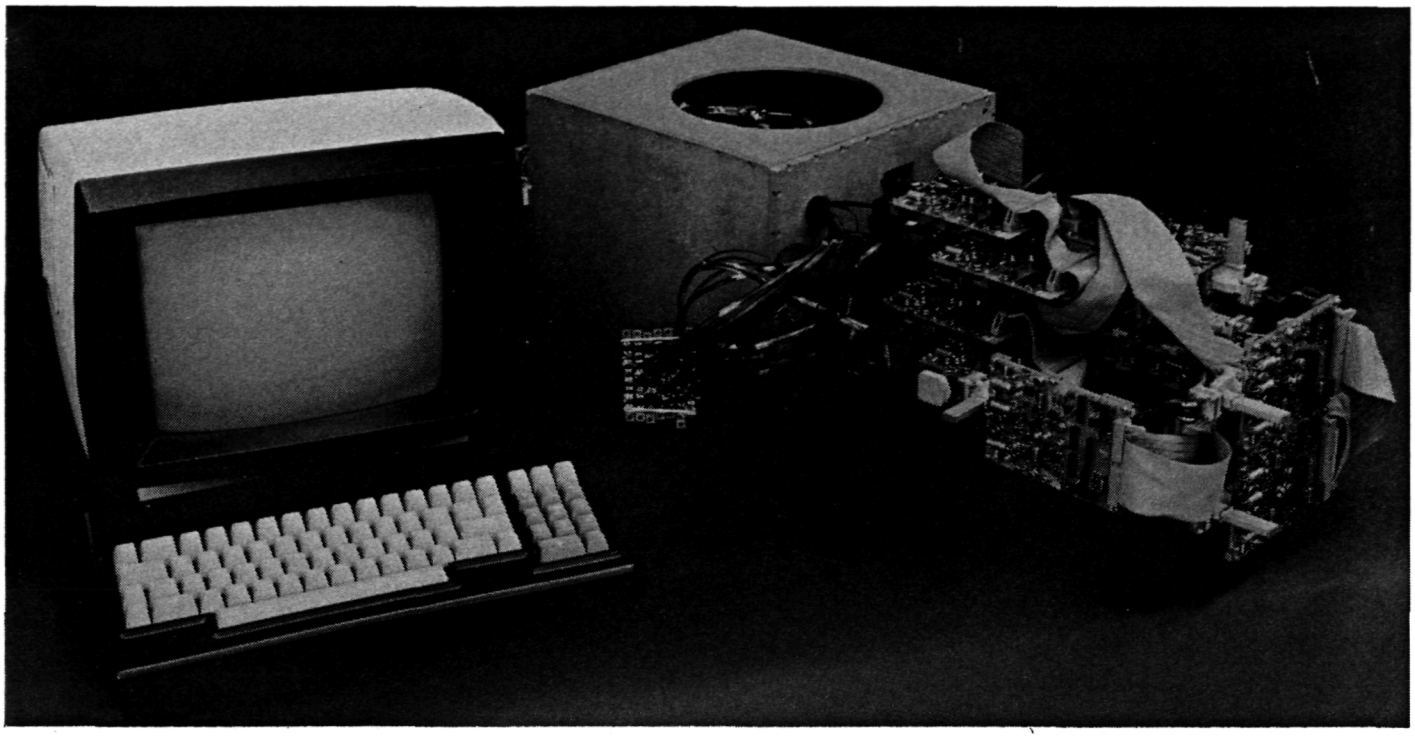

Figure 4.8 Scan Beamforming Network and Controller

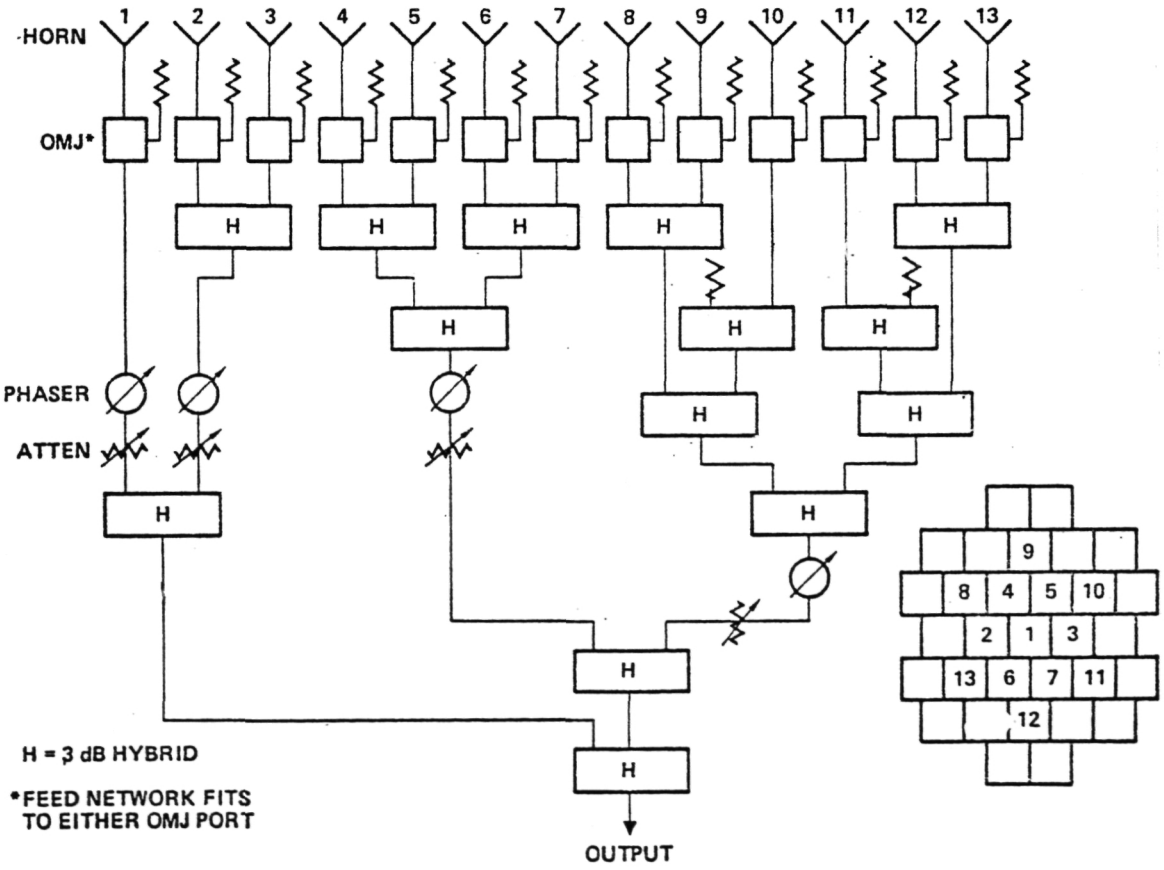

Figure 4.9 POC BFN Configuration - Trunk Fixed Beams

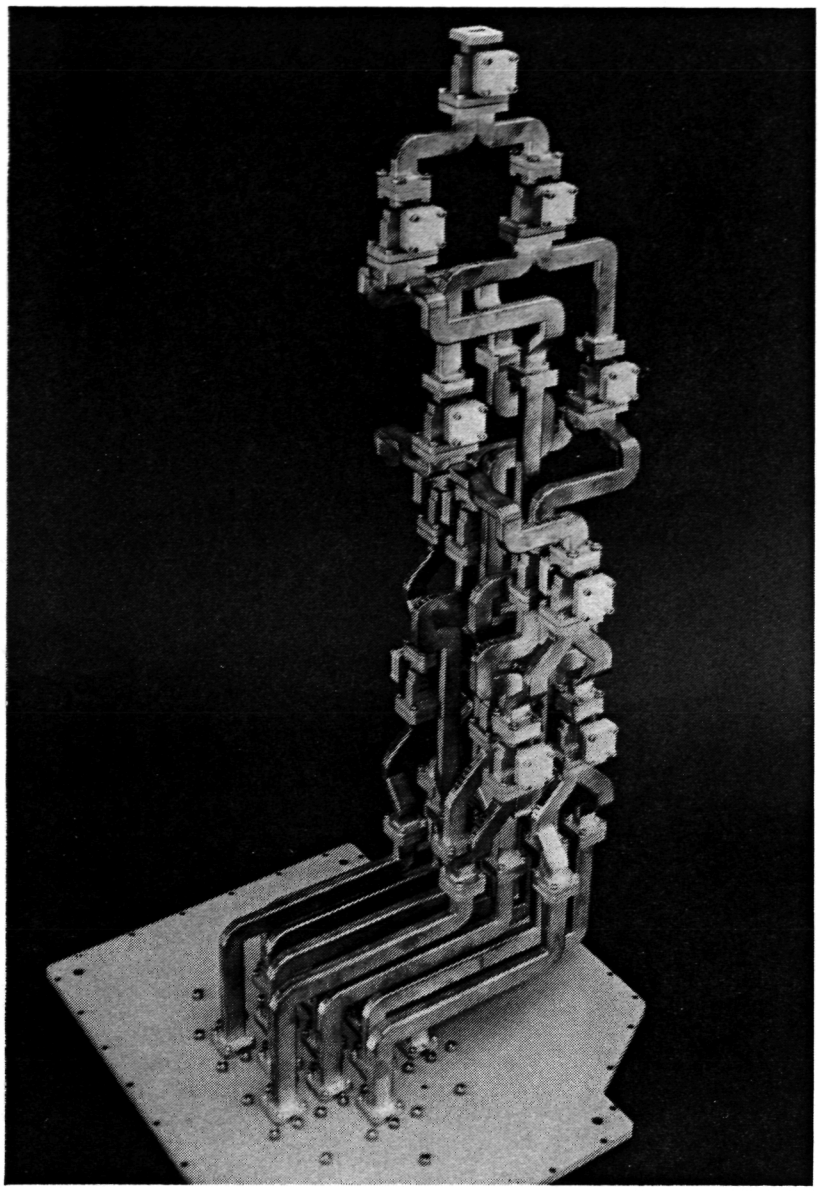

Figure 4.10 Trunk Beam Network

5.0 Proof-of-Concept Model Tests

The primary goal of the POC model test program has been to measure and analyze the Multiple Beam Antenna System performance characteristics, including beamshape, sidelobe levels, gain and beam pointing direction. To reach this goal extensive component and subsystem testing has been required as well as final system testing on the pattern range.

The analysis of the range results is mainly a comparison of measured and calculated results, and the general agreement between these is excellent. This correlation is more important because it means that performance of any similar satellite antenna system can be predicted by calculation and that system checkout of any such MBA will not require direct measurement of every electromagnetic feature.

In the remainder of this section the subsystem tests are discussed, starting with laboratory tests and concluding with range tests.

5.1 Laboratory Tests Laboratory measurements were made on all components and sub-assemblies including the complete feed arrays and network. Some units were tested by the manufacturer and only checked by FACC, but all were tested. Only tests for the scan beam assembly are discussed here, however.

5.1.1 Scan Beam Network Tests

The scan beam network testing included calibration of individual VPD's and VPS's and the total network, as well as measurements of losses for all individual components.

Insertion losses of the entire BFN and of the sub-assemblies were also measured. The results are given in Table 5.1.

Table 5.1

Scan Network Measured Insertion Loss

Switch Matrix	0.60 dB
VPD's 3 x 0.55	1.65 dB
VPS	0.67 dB
Sum	2.92 dB
Measured Total	3.12 dB

Measured individual VPD attenuation deviations from set values were quite small; the average being 0.26 dB, and the error in VPS phase settings averaged only 1.6 degrees. These components, therefore, appear to be entirely adequate for this

network application. It should be mentioned, however, that VPD No. 1 did have an abnormally high error of about 0.5 dB.

This VPD No. 1 was replaced with a spare for the horizontal polarization range tests so that better amplitude control would be available. It turned out that this change introduced a 30 degree phase difference in half of the cluster horns. Recalibration for phase was done before the vertical polarization range tests were made, so this phase error was not present in those tests.

During the course of testing, one VPD apparently failed and was temporarily replaced with a spare. Further investigation showed that the failure was intermittent and was probably caused by a poor cable connection.

The ferrite components were subjected to power testing. These tests showed that at room temperature the circulator switches could handle at least 40 watts and the phase shifter could handle at least 15 watts.

5.1.2 Scan Beam Array Tests

Primary pattern measurements, made in an anechoic chamber lined with absorbing material, show that even though there was reasonable agreement between measured and calculated primary patterns there were some discrepancies for the 7 horn cluster. These are:

- At 19.1 GHz the E-plane main beam peak is flattened.
- The measured H-plane grating lobe is about 2 dB larger than the calculated value.

Both effects may be a result of mutual coupling between adjacent horns which is not considered in the calculating program. These effects should have a negligible effect on the secondary beam shape, but there may be a slight loss of gain caused by the larger grating lobe, the extra energy in the grating lobes is energy that misses the main reflector and is therefore lost. For a flight system design it would be best to use the measured primary patterns in the secondary patterns calculating program.

A photograph of the indoor range and test equipment is shown in Figure 5.1.

5.2 Antenna Range Tests

Antenna pattern and gain measurements were made for horizontal and vertical polarization on the FACC Building One to Black Mountain Antenna Range during the months of April to August 1983. Prior to the actual antenna measurements, aperture field probe data was acquired and analyzed to evaluate the

potential effects of ground reflections. It was concluded that the MBA's narrow beam would provide sufficient discrimination to make ground reflected energy negligible for areas of interest.

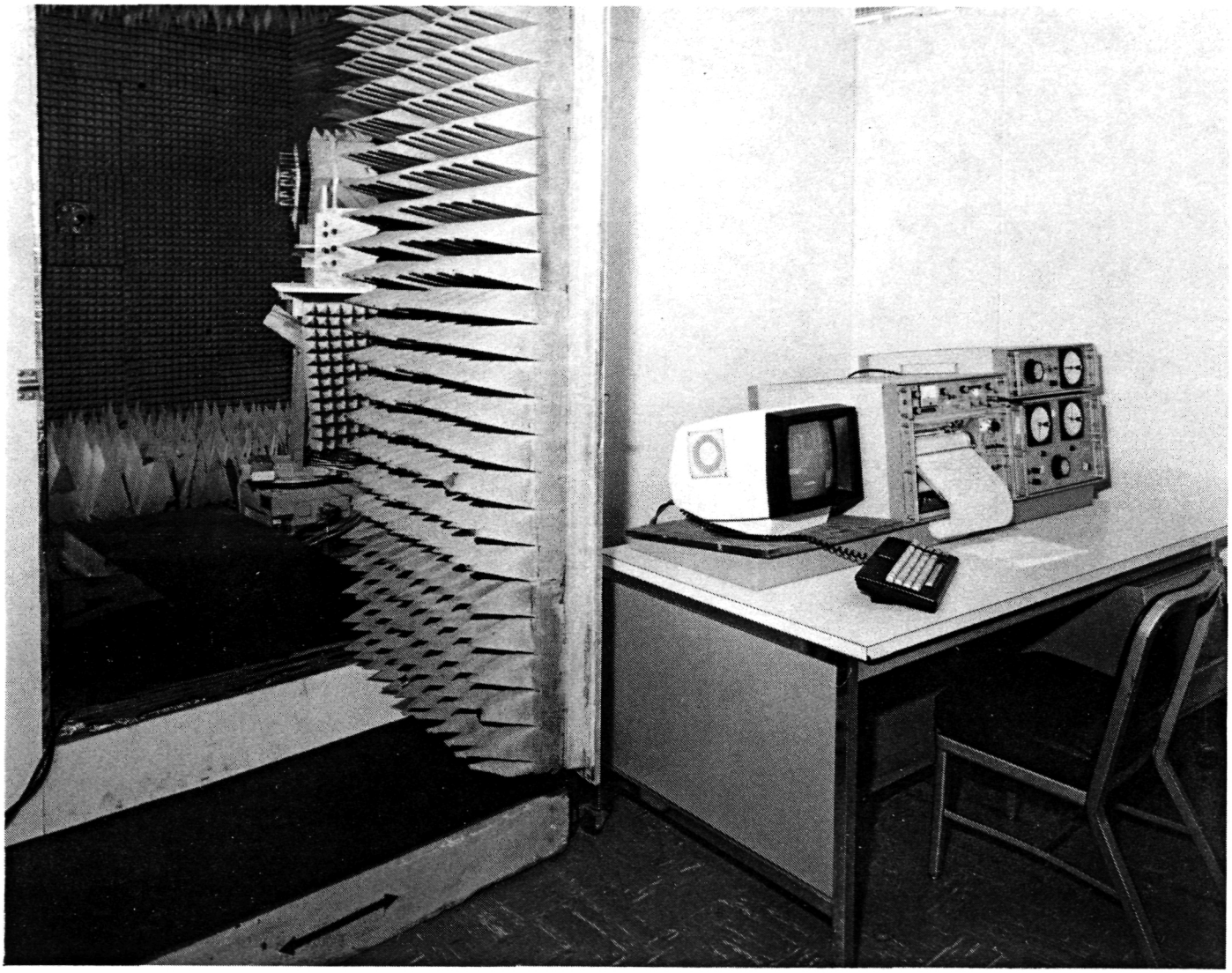

Figure 5.1 Indoor Range & Test Equipment

On some days weather conditions did cause such rapid signal variation that is was impractical to operate effectively. This fading was most likely caused by wave interference brought about by vertical atmospheric stratification. Most of the time, measurements were repeatable with remarkably close agreement to calculated patterns and gains, however.

The following pages describe range equipment and general procedures and also presents measured results with comparable calculated data.

5.2.1 Range and Equipments

The range profile is displayed in Figure 5.2, and Table 5.2 lists the key range parameters. As mentioned above, analysis confirmed that reflected energy should not cause a problem.

A block diagram and a list of key features for the antenna measuring system are given in Figure 5.3. In addition, it should be mentioned that the pedestal provides for making measurements by either azimuth or elevation rotation and for setting the MBA to any desired axial position.

The scan beam controller may be used to set in any one of 14 beams. The relative amplitude and phase for each of the seven cluster elements are electrically adjustable by setting the VPD's and VPS's. The Scan Beam Operating Manual for Control Electronics, Ref. 10 of Appendix B includes a description of the beam controller system

A photograph of the Scientific Atlanta pattern recording equipment is shown in Figure 5.4.

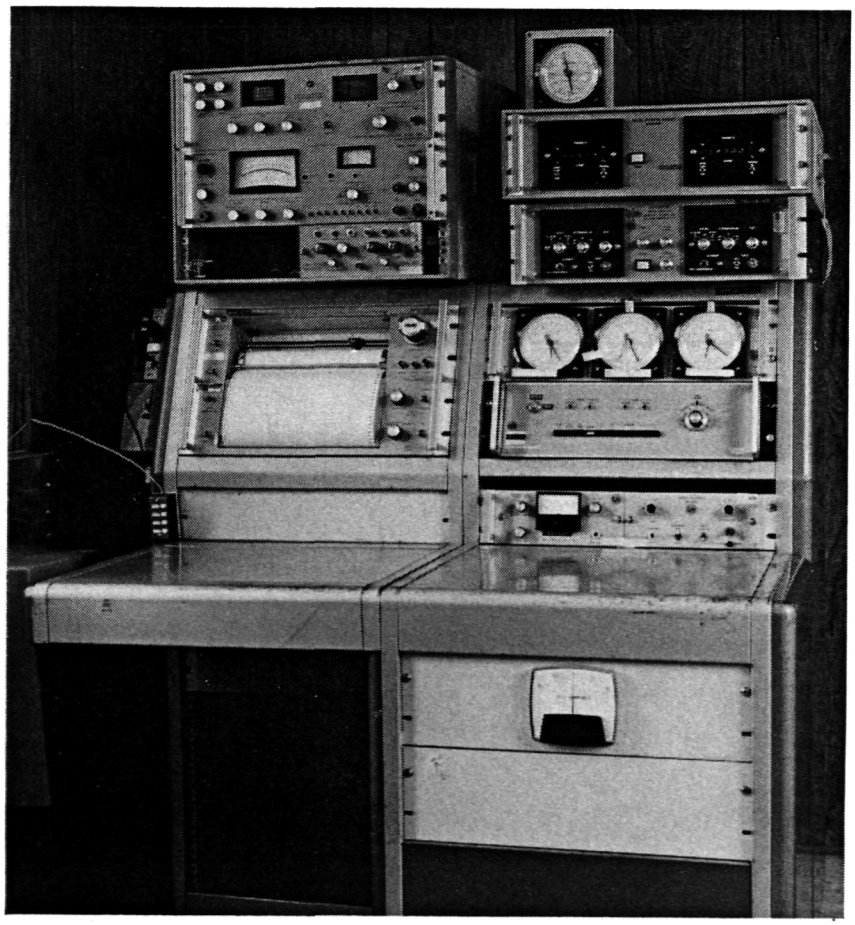

Figure 5.4 Range Recording Equipment

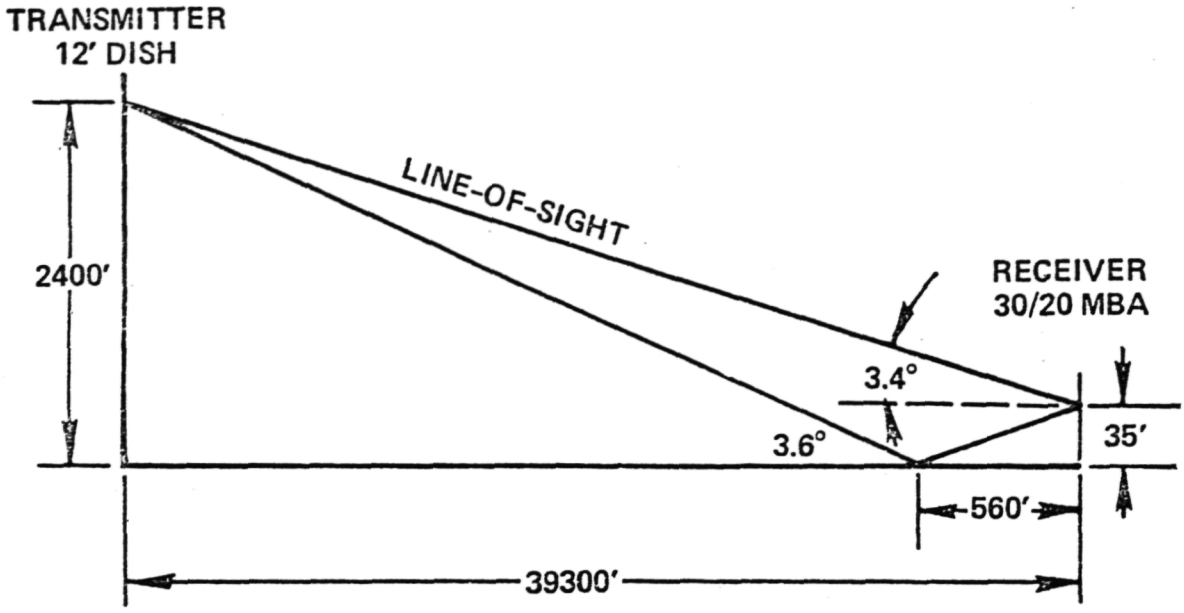

Figure 5.2 Antenna Test Range

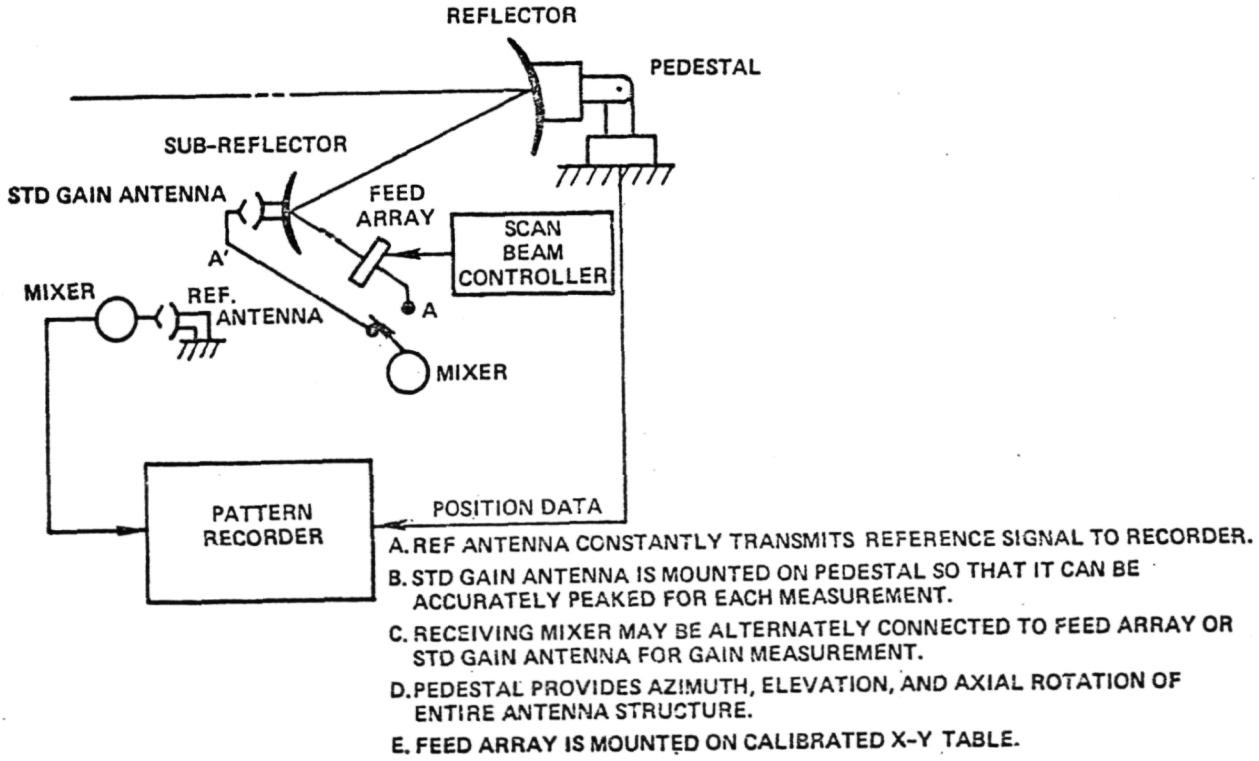

Figure 5.3 Schematic Diagram for Antenna Tests

5.2.2 Installation and Alignment of the MBA

During installation great care was taken to follow a precisely defined procedure for lifting and placing each component so that no unknown distorting strains were developed. For proper performance it was also required that the three components, main reflector, subreflector and feed array be accurately aligned. This alignment was accomplished by use of a centrally located theodolite for measuring the angular positions of the various fiducial marks on the three components.

The tubular steel support structure does deflect under gravity loading for different axial positions. To measure these deflections three lasers with targets were included for dynamic alignment measurement. It turned out, however, that the major effect of the dynamic deflections was to change beam pointing direction with an insignificant distortion of the beam pattern. The lasers were actually an unncessary precaution.

The measured patterns imply that the installation and alignment procedures were satisfactory.

Table 5.2

RANGE PARAMETERS

Wavelength (nominal)		0.6 in = 0.05 ft
Transmitting antenna diameter		12 ft
MBA diameter		13.5 ft
Beam widths (Xmtr = Rec)		0.3°
Range, R		39,300 ft
Angle subtended by MBA		1/14 BW
Phase error - $D^2/8R$	0.012	$= 4.2^{\circ}$
Specular reflection angle		25 BW (7°)

5.3 Test Program

The front view and side view of the test antenna system are given in Figure 4.1. The feed array contains 32 loaded horns and 24 dummy horns. Figure 5.5 illustrates the feed array layout. Thirty two horns are numbered by a number at top, left corner of each horn. Fourteen numbers in parenthesis indicate the numbering of 14 beams. The feed array may be set electrically to 14 single beams and 14 cluster beams by use of the remote scan beam controller (EMS controller) located near

the pattern recorder. For convenience, a single digit or a double digit number (for example, # 9) refers to a 7-horn cluster beam, and a three digit number (for example, # 109) refers to a single horn beam. To be specific, beam # 9 would make use of seven horns, #14, #15. #18, #19, #20, #23, and #24. Beams #109 would make use of feed horn #19 only.

The feed array is mounted on the feed rack, an X-Y table, which may be set to any precise position within the range limits (∓ 10 pitches in y direction and ∓ 14 pitch in X direction). Thirteen typical array position, as shown in Figure 5.6 are selected for the test measurement. For convenience, a shorthand abbreviation (X,Y) for each mechanical position is used. For example (14,-10) represents the array position which is 14 pitches in the positive X direction and 10 pitches in the negative y direction. Beam #9 and Beam #109 were measured for all 13 array positions. Other beams were also measured whenever it is desired.

A pattern measurement flowchart is given in Figure 5.7. The feed array can be moved to a desired position by using the horizontal and vertical cranks. For a cluster beam, a set of theoretical excitation coefficients (amplitude and phase) is converted into VPD and VPS command settings. We input the settings into the EMS controller to set the antenna to the desired beam. For a single horn beam, no coefficients would be needed, all but a single central horn are attenuated.

In general, patterns are measured by azimuth and elevation rotation with changes to horizontal, vertical or other orientations made by axial rotation of the MBA about the line of sight axis. The co-pol pattern is measured with the transmitter polarization oriented for maximum signal level at beam peak. For cross-pol patterns, the polarization orientation is for minimum signal level at beam peak. This latter orientation is approximately 90 degrees from the first. The direction of a beam peak is calculated by a computer program. Nevertheless, in most cases, the operator can locate the beam peak rather easily by manually adjusting aximuth and elevation angles.

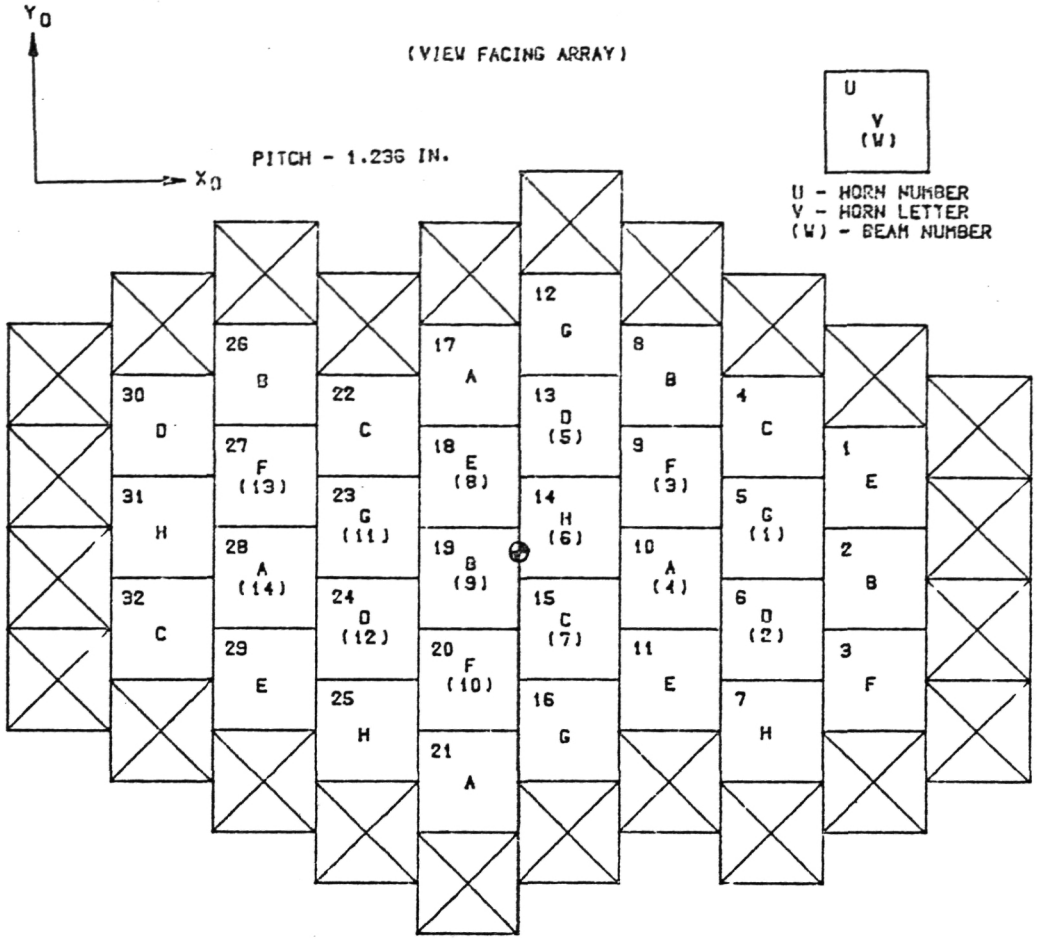

Figure 5.5 Feed Array Layout

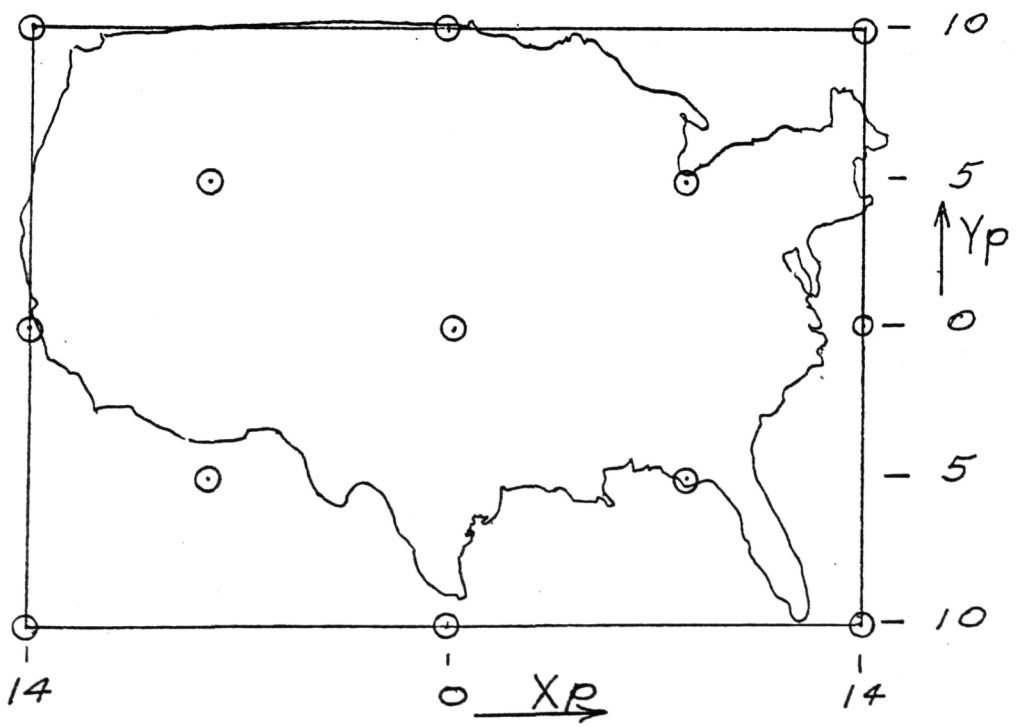

X_p, Y_p in pitches; 1 Pitch = 1.236 inch

Figure 5.6 The 13 Key Array Positions

An azimuth pattern is measured by scanning the MBA from left to right. The right portion of the azimuth pattern is recorded on the right hand side of the paper. An elevation pattern is measured by scanning the MBA from bottom to top. The top portion of the elevation pattern is recorded on the right hand side of the paper.

Typical patterns for horizontal polarization are shown in Figures 5.8 to 5.16. In these figures, theoretical patterns shown as small circles have been added to the measured patterns. A perfect agreement between measured and calculated azimuth patterns for beam #109 at position (0,0) is shown in Figure 5.8. Figure 5.9 shows the measured elevation pattern for beam #109 at position (0,0) deviates slightly from its corresponding calculated pattern in sidelobe positions. Note that patterns measured by elevation rotation always incur more ground reflections than that measured by azimuth rotation. Since an azimuth pattern at 90 degrees axial rotation is the same pattern as the elevation pattern at normal position (0° axial rotation), we rotated the MBA to its 90° axial rotation and measured the azimuth pattern. Figure 5.10 shows the comparison between the azimuth pattern measured at 90° rotation to the caluclated elevation pattern. The excellent agreement between the two verifies that the deviation in sidelobe structure for a elevation pattern was caused by ground reflection.

Figure 5.11 shows the comparison for 45° plane pattern. Other than a slightly flat top of the main beam for the measured pattern, excellent agreements are observed between the two. The flat top of main beam could be caused by signal fluctuations.

Figure 5.12 shows azimuth pattern of beam # 9 at position (0,0). The pattern has a 20 dB width of 0.59° and first sidelobe of 26.1 dB. Figure 5.13 shows elevation pattern of beam # 9 at position (0,0). The pattern has a 20 dB width of 0.66° and first sidelobes of 30 dB. Figure 5.14 shows a comparison between the measured 45° pattern of beam # 9 for (0,0) position at 19.1 GHz and its theoretical counterpart. Clearly, an excellent agreement between the two is observed.

Figure 5.15 shows azimuth pattern of beam # 9 at position (14, 10). The comparison indicates that the measured pattern has a slightly higher sidelobe. Figure 5.16 shows elevation pattern of beam #9 at position (14, 10). The comparison indicates that the measured pattern has a slightly broader mainbeam.

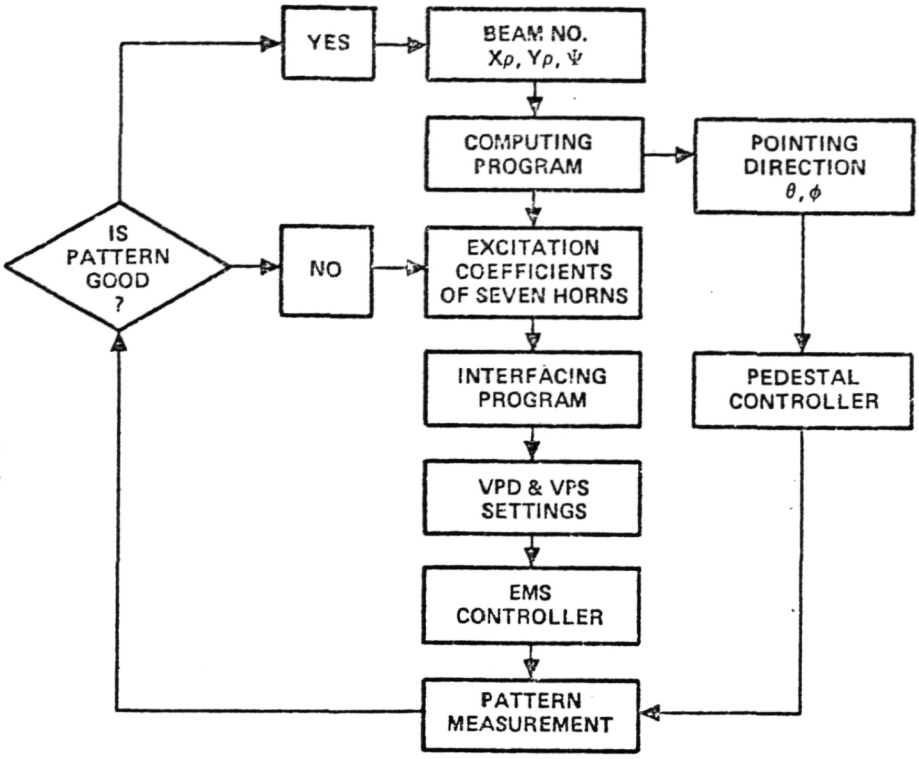

Figure 5.7 Pattern Measurements Flowchart

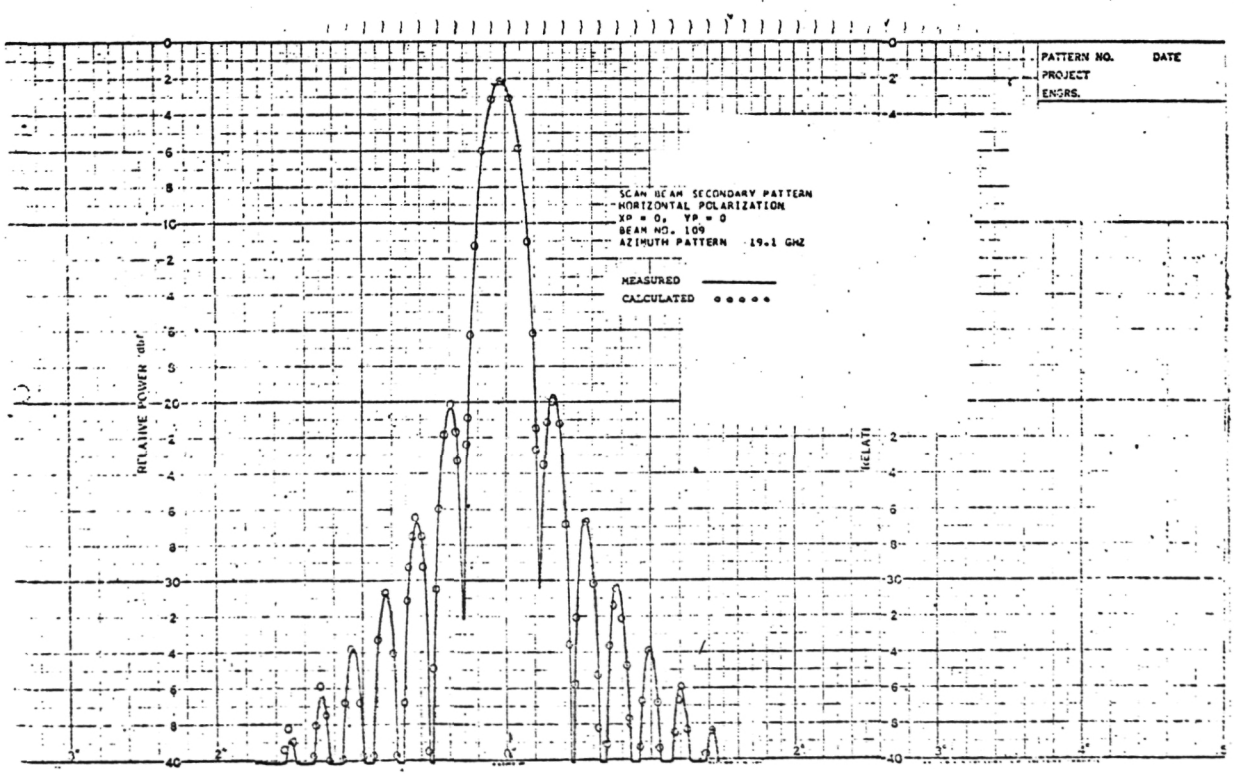

Figure 5.8 Beam #109, Azimuth Pattern Horizontal Polarization Position (0,0)

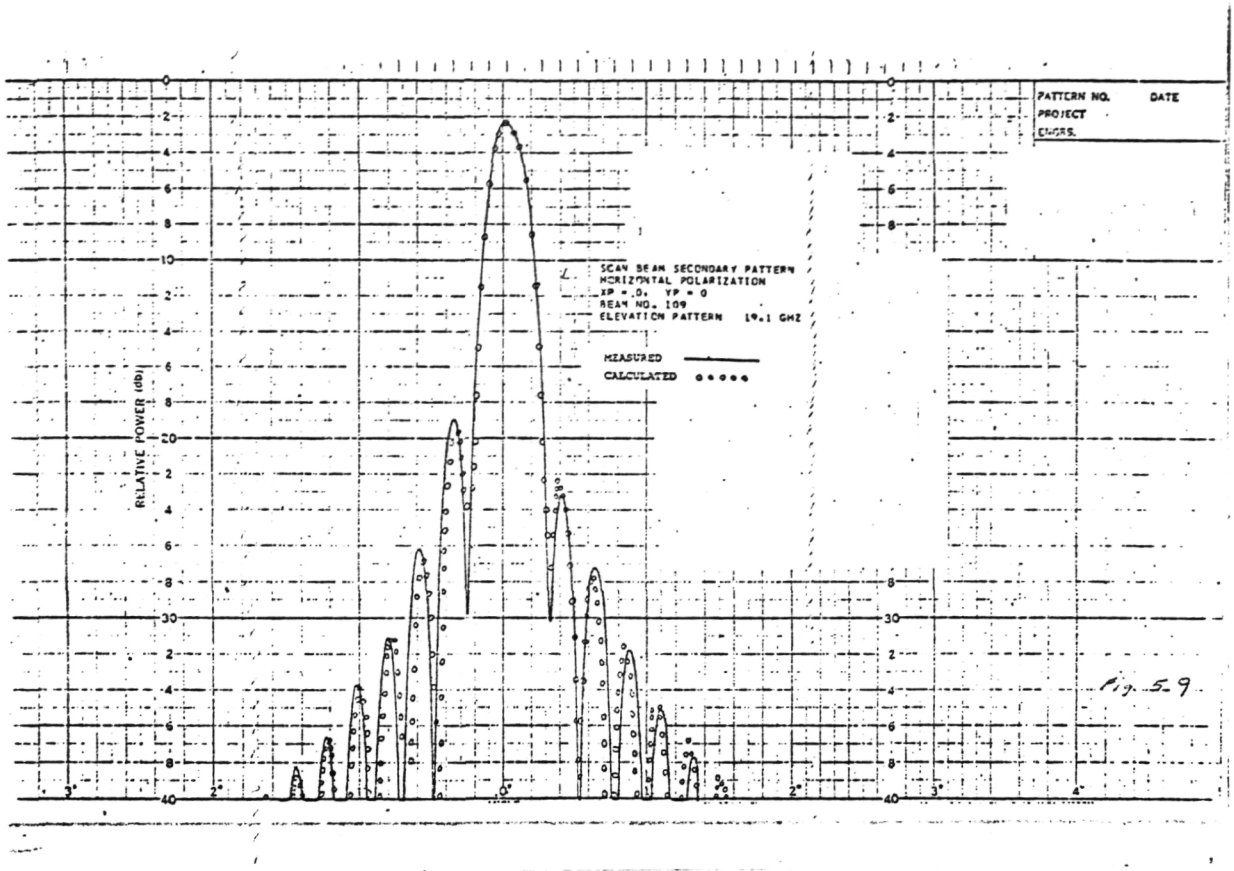

Figure 5.9 Beam #109, Elevation Pattern Horizontal Polarization Position (0,0)

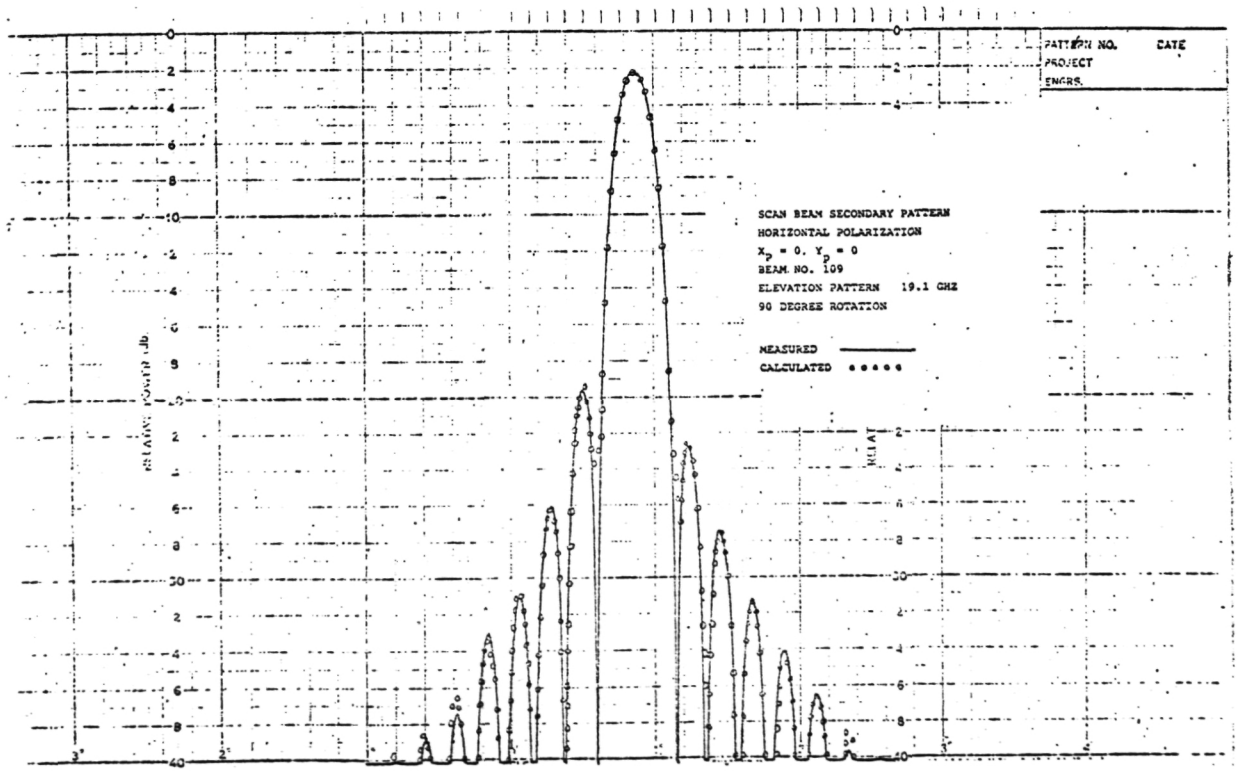

Figure 5.10 Beam #109, Elevation Pattern Horizontal Polarization (0,0), 90^{O} Rotation

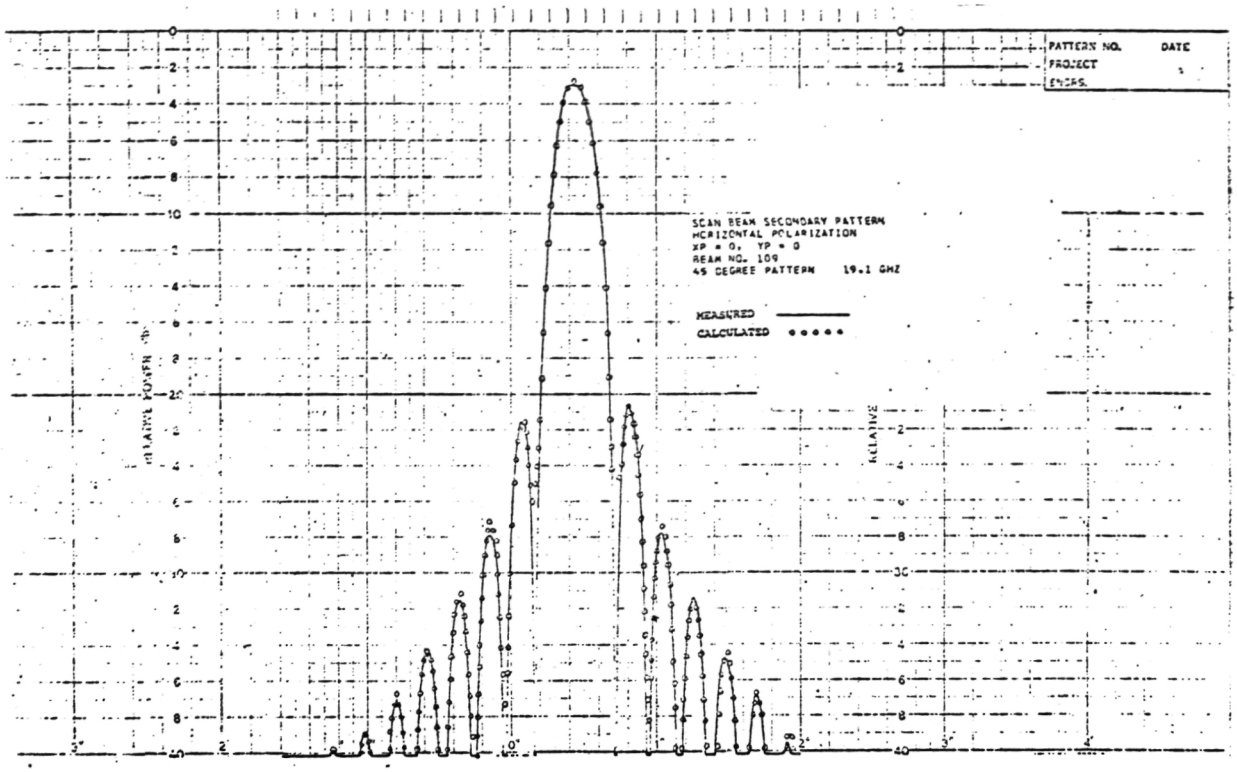

Figure 5.11 Beam #109, 45° Pattern Horizontal Polarization Position (0,0)

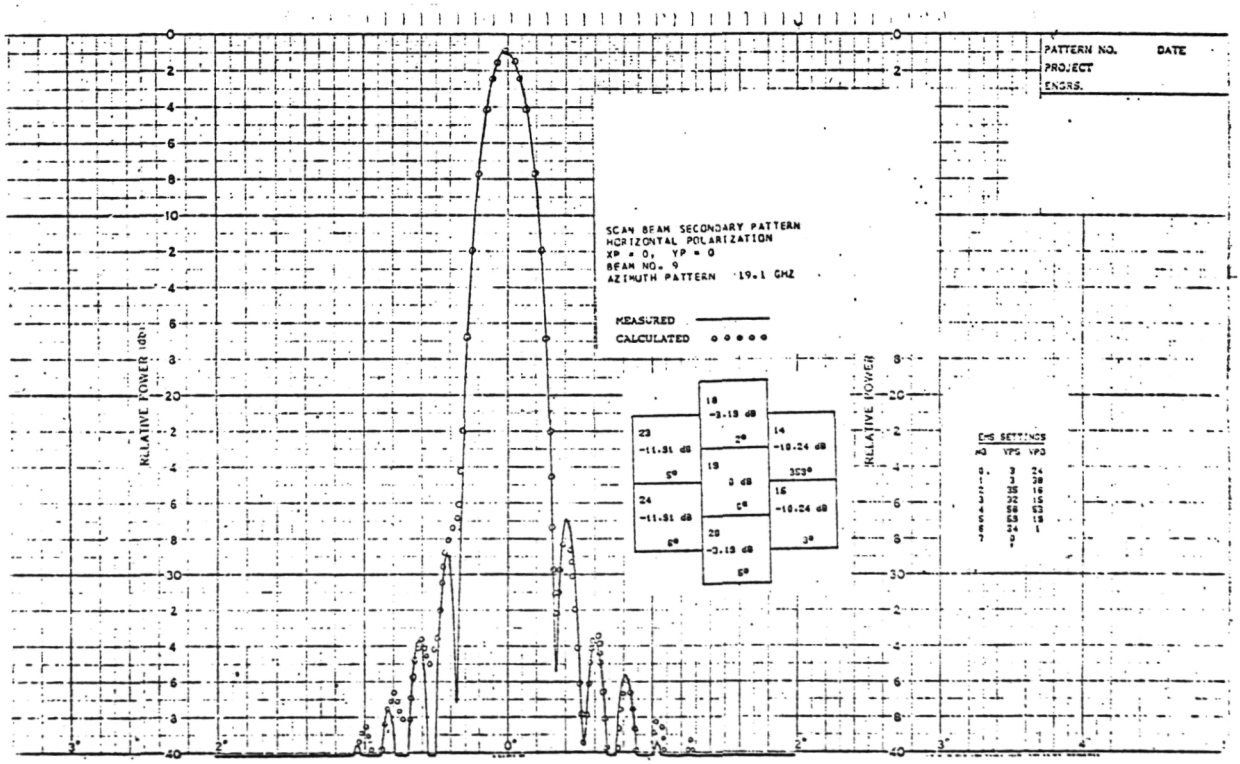

Figure 5.12 Beam #9, Azimuth Pattern Horizontal Polarization Position (0,0)

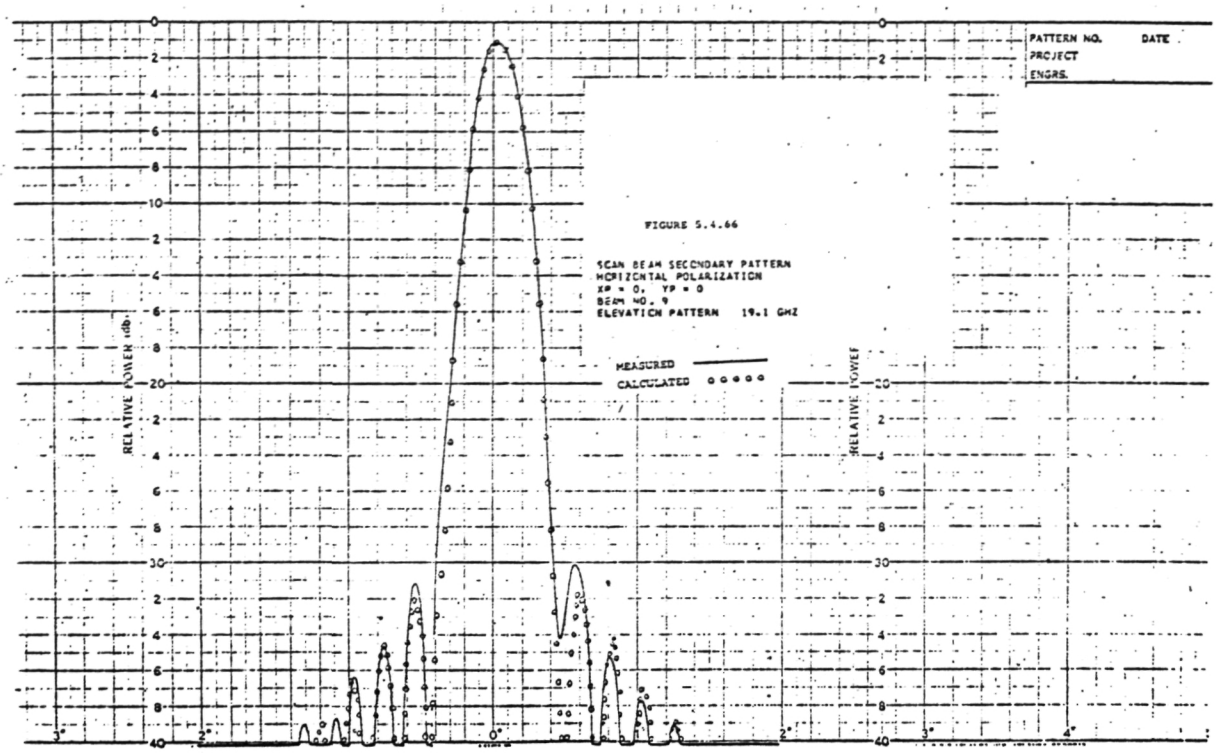

Figure 5.13 Beam #9, Elevation Pattern Horizontal Polarization Position (0,0)

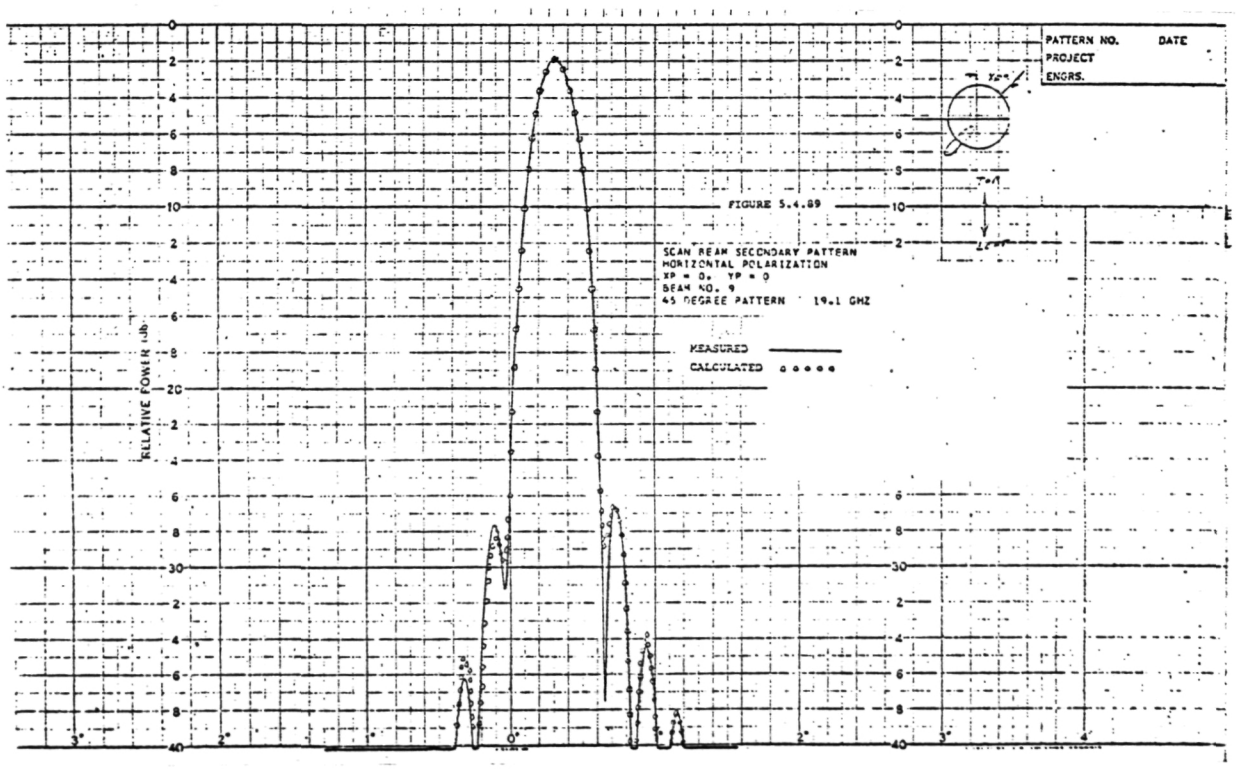

Figure 5.14 Beam #9, 45° Pattern Horizontal Polarization Position (0,0)

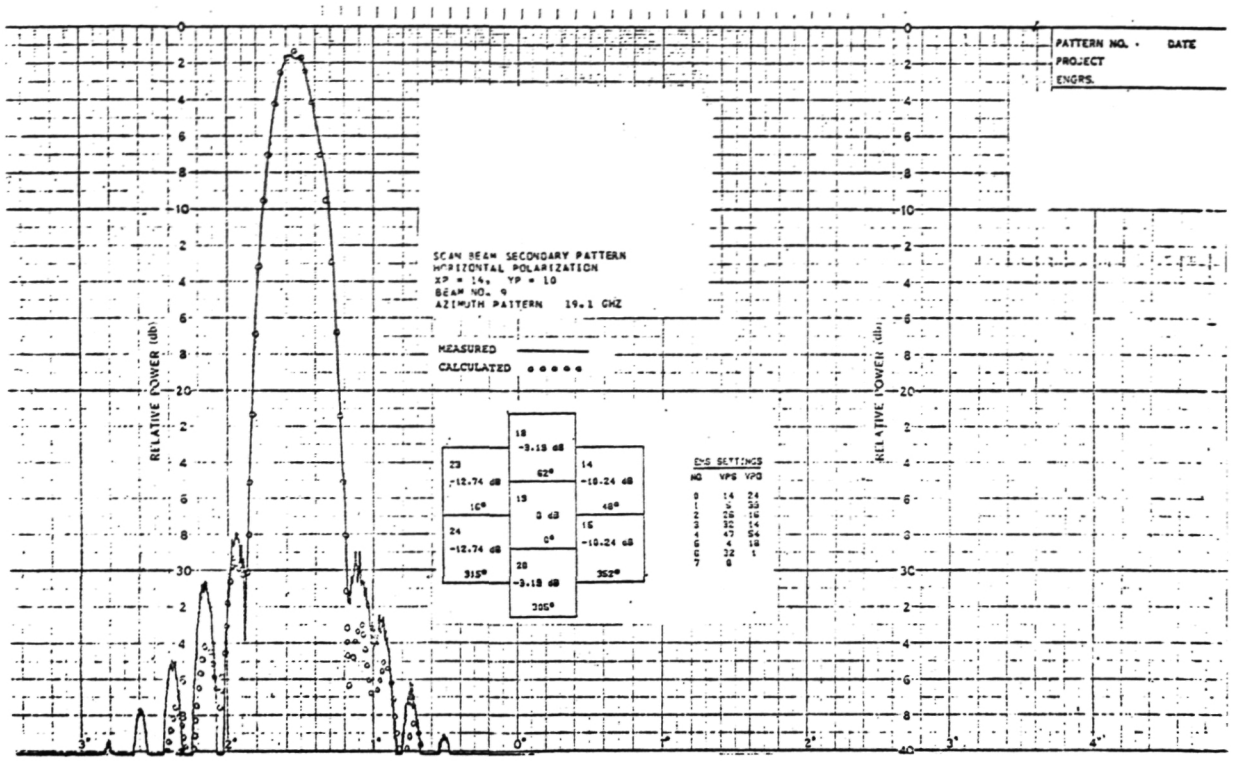

Figure 5.15 Beam #9, Azimuth Pattern Horizontal Polarization Position (14,10)

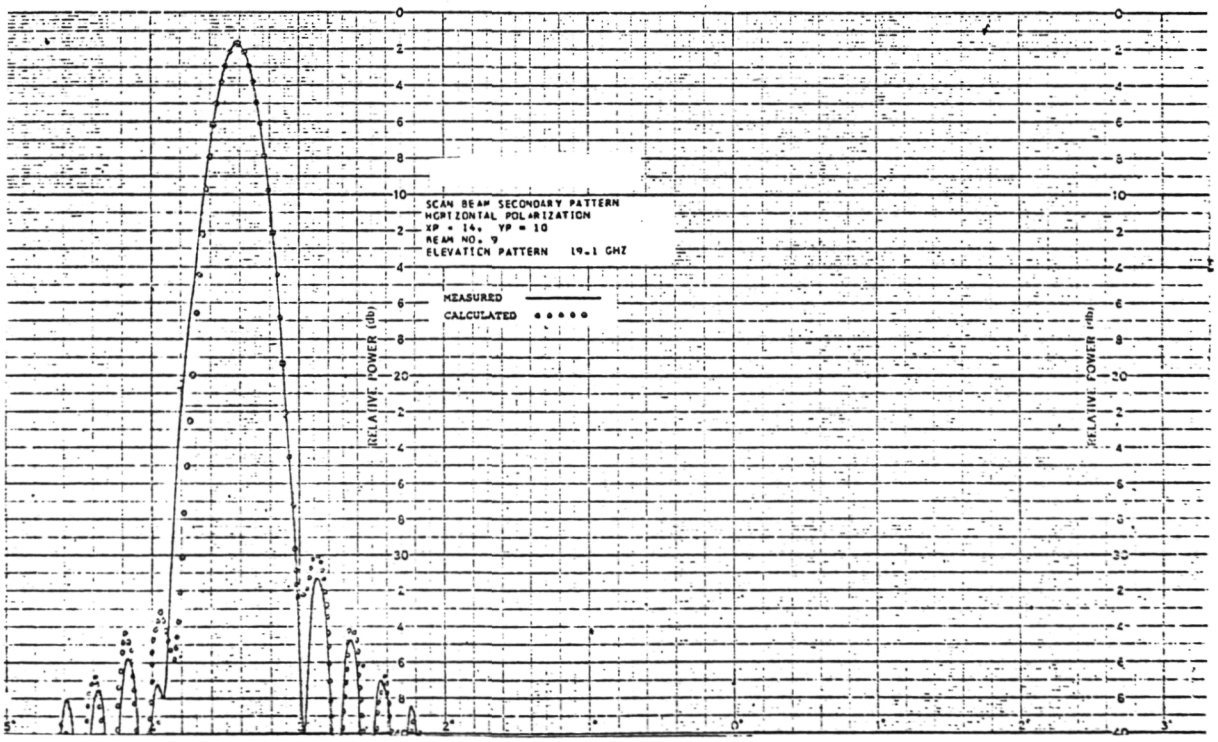

Figure 5.16 Beam #9, Elevation Pattern Horizontal Polarization Position (14,10)

Typical patterns for vertical polarization are shown in Figures 5.17 to 5.21. Figure 5.17 shows azimuth pattern of beam #9 at position (0,0). The pattern has a 20 dB width of 0.58^{o} and first sidelobe of 26.2 dB at 19.1 GHz. Figure 5.18 shows elevation pattern of beam #9 at position (0,0). The pattern has a 20 dB width of 0.73^{o} and first sidelobe of 30 dB. Figure 5.19 shows a comparison between the measured 45^{o} pattern and the calculated 45^{o} pattern of beam #9 at (0,0) position. An excellent agreement between the two is observed. Figure 5.20 shows azimuth pattern of beam #9 at position (-14,10). The comparison indicates that the measured pattern has a narrower mainbeam. Figure 5.21 shows elevation pattern of beam #9 at position (-14,10). Again, the comparison indicates that the measured pattern has a narrower mainbeam.

Antenna gain is measured by the conventional substitution method. A schematic diagram of the gain measurement is given in Figure 5.22. This is accomplished by switching the same assembly of mixer, isolator, and cable from the test antenna (MBA) to a calibrated standard gain antenna. An additional 9.7 dB pad is used for the test antenna in order to reduce the output level difference between the test antenna and the standard gain antenna. The standard gain antenna, calibrated by NATIONAL STANDARD BUREAU, has 43.54 dB gian with + 0.17 dB uncertainty at a frequency 19.1 GHz. The feed network has 3.15 dB loss at 19.1 GHz for both single-horn beam and seven-horn cluster beam. As a result, for each gain measurement, we have

Gain =	Standard Ant. Gain	+	Pad Attenuation	+	Network Loss	- Power Level Difference Betweem Test Antenna and Standard Antenna

Gain measurements at on-axis and four corner positions for horizontal polarization are summarized in Table 5.1. Gain measurements at on-axis and four corner positons for vertical polarization are summarized in Table 5.2.

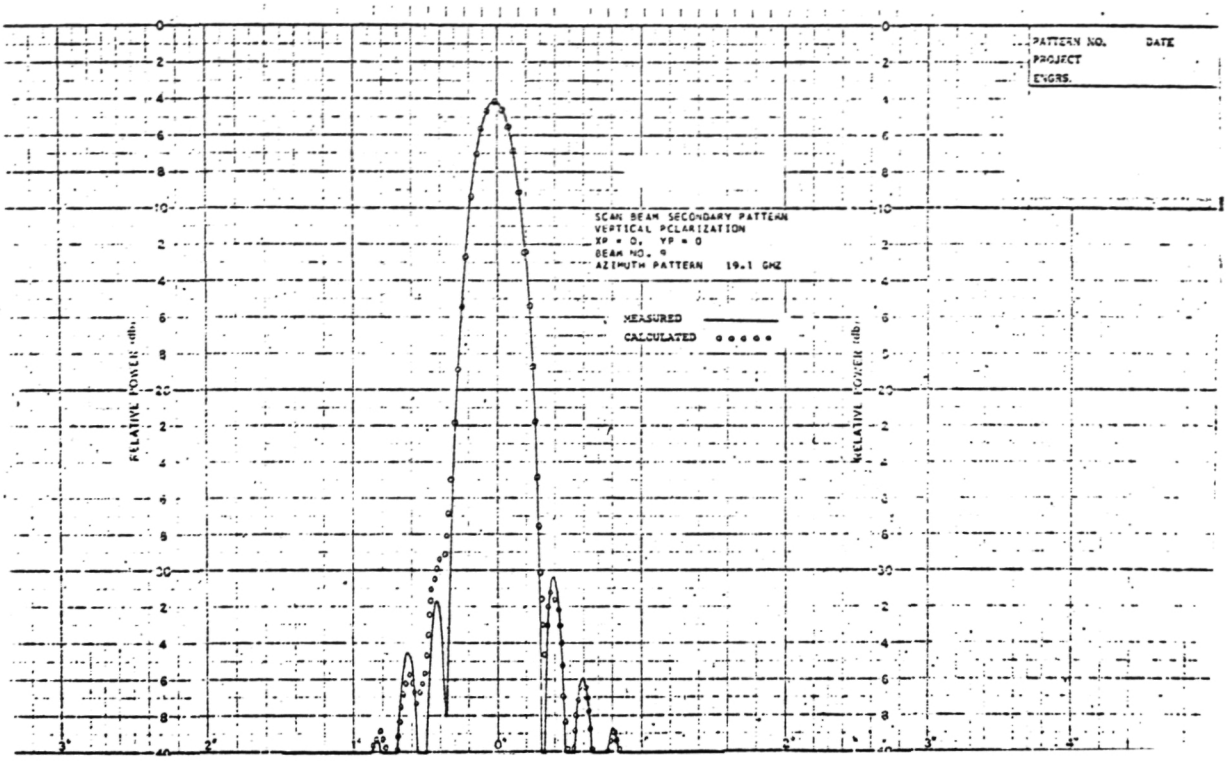

Figure 5.17 Beam #9, Azimuth Pattern Vertical Polarization Position (0,0)

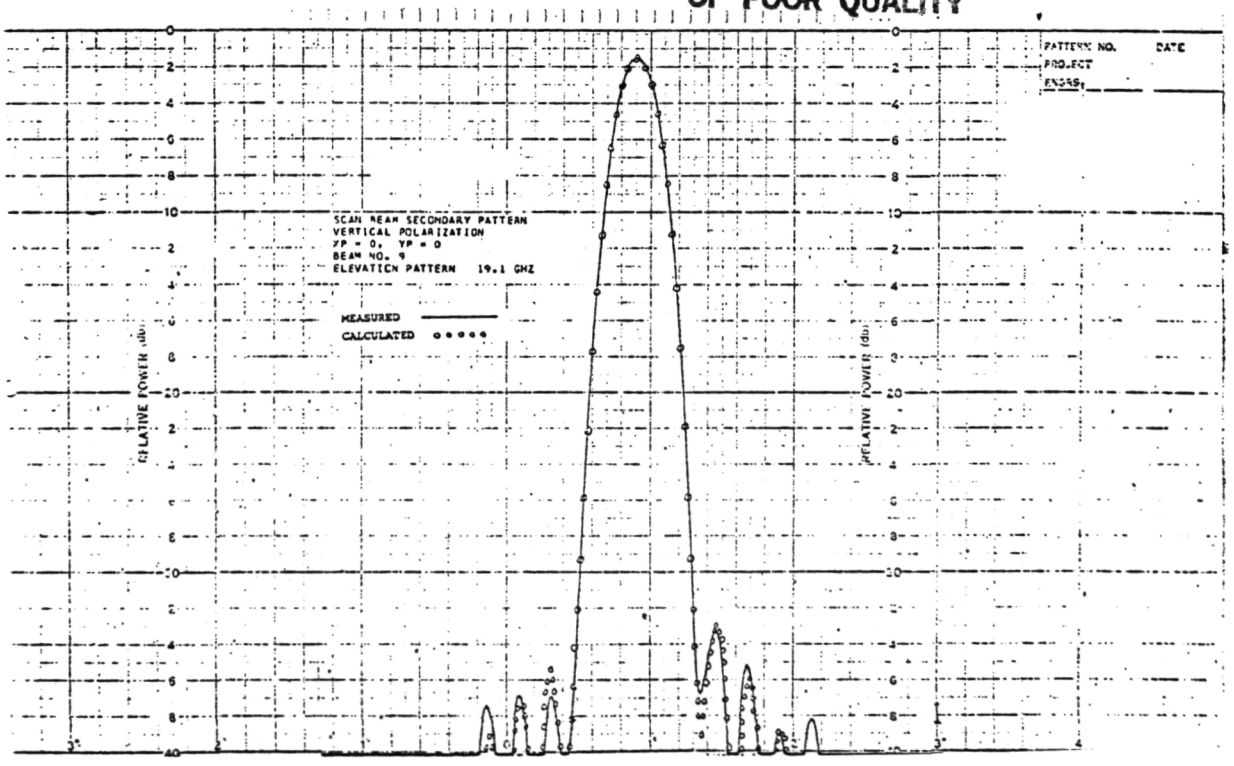

Figure 5.18 Beam #9, Elevation Pattern Vertical Polarization Position (0,0)

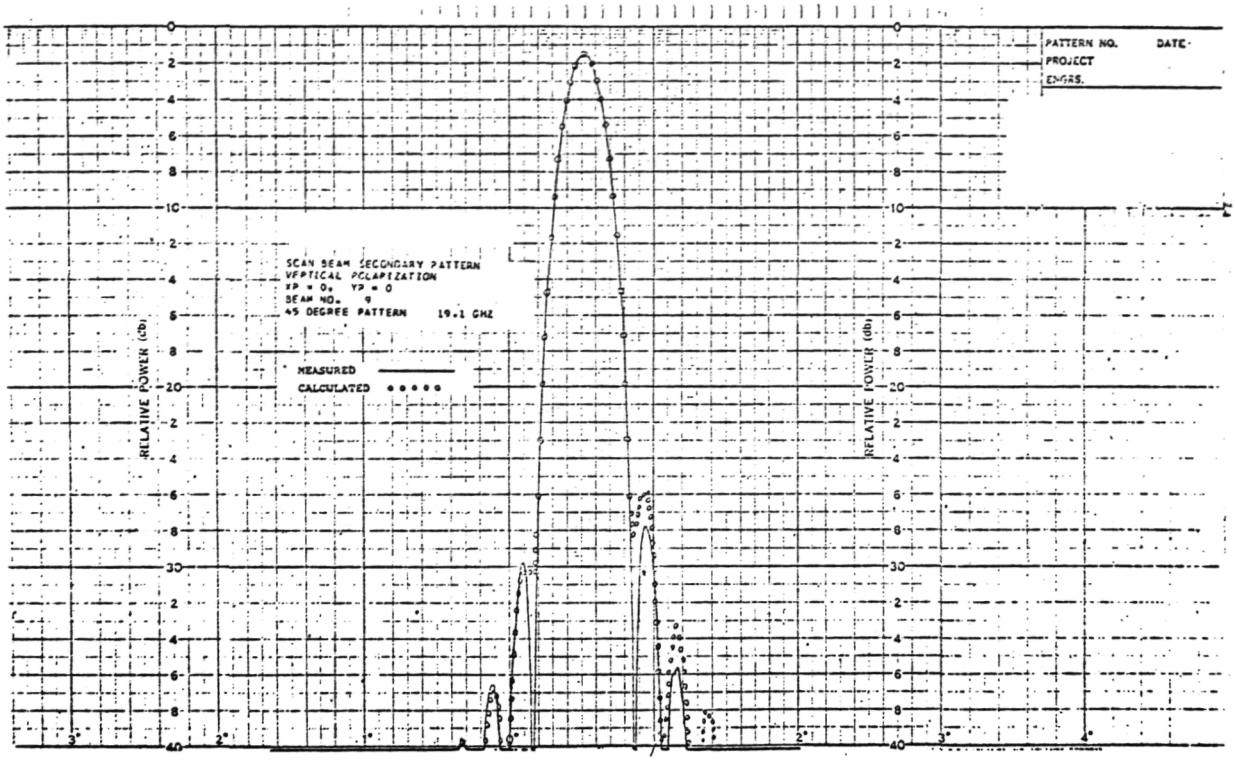

Figure 5.21 Beam #9, 45° Pattern Vertical Polarization Position (0,0)

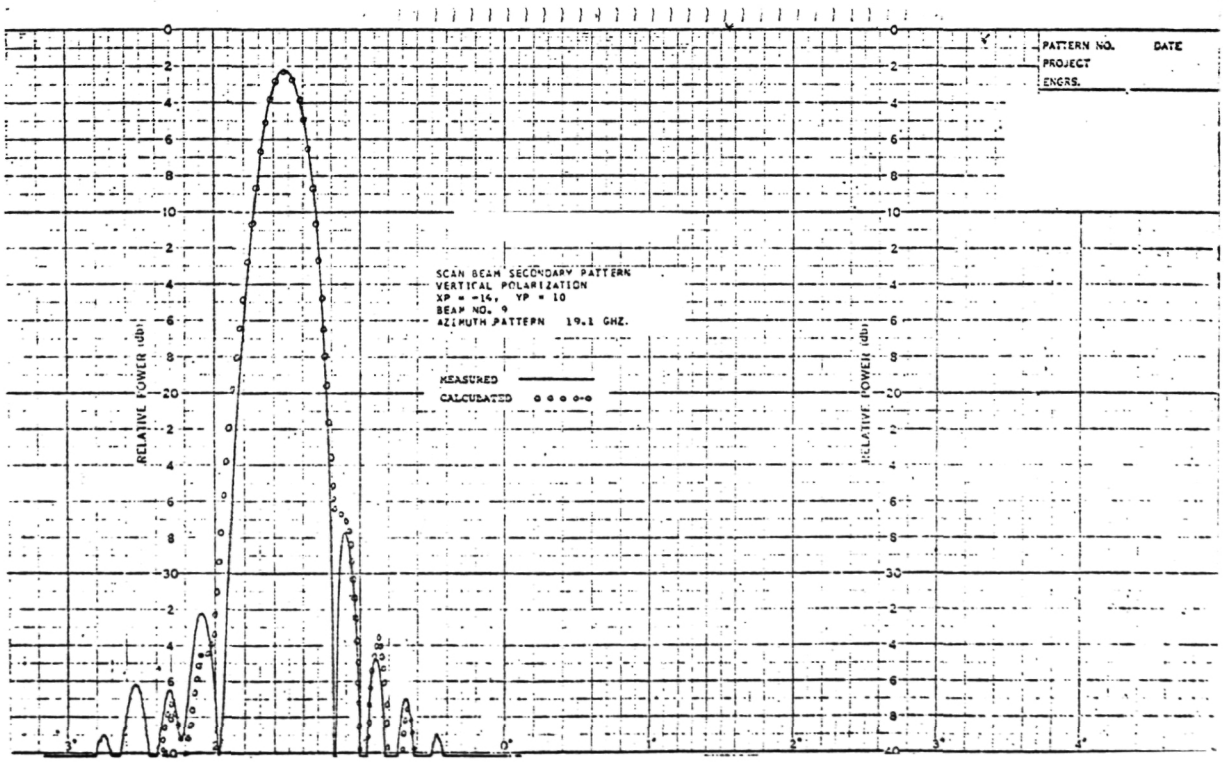

Figure 5.20 Beam #9, Azimuth Pattern Vertical Polarization Position (-14,10)

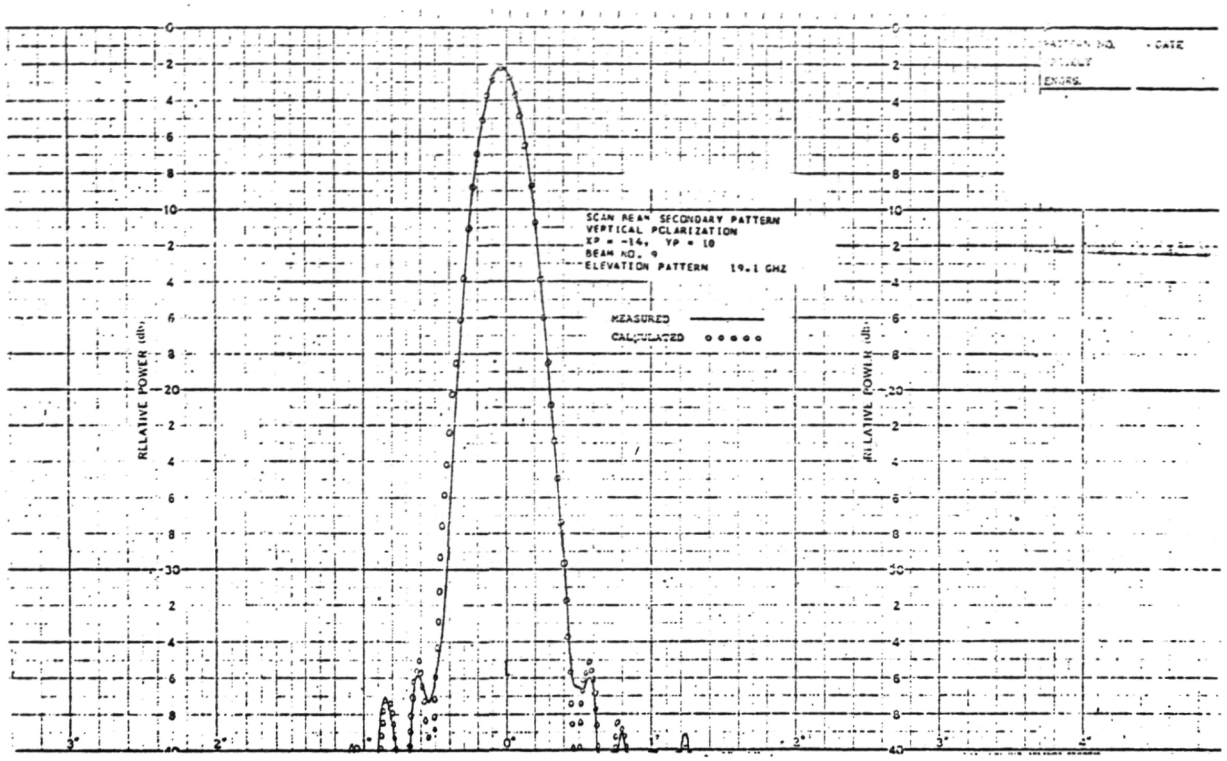

Figure 5.21 Beam #9, Elevation Pattern Vertical Polarization Position (-14,10)

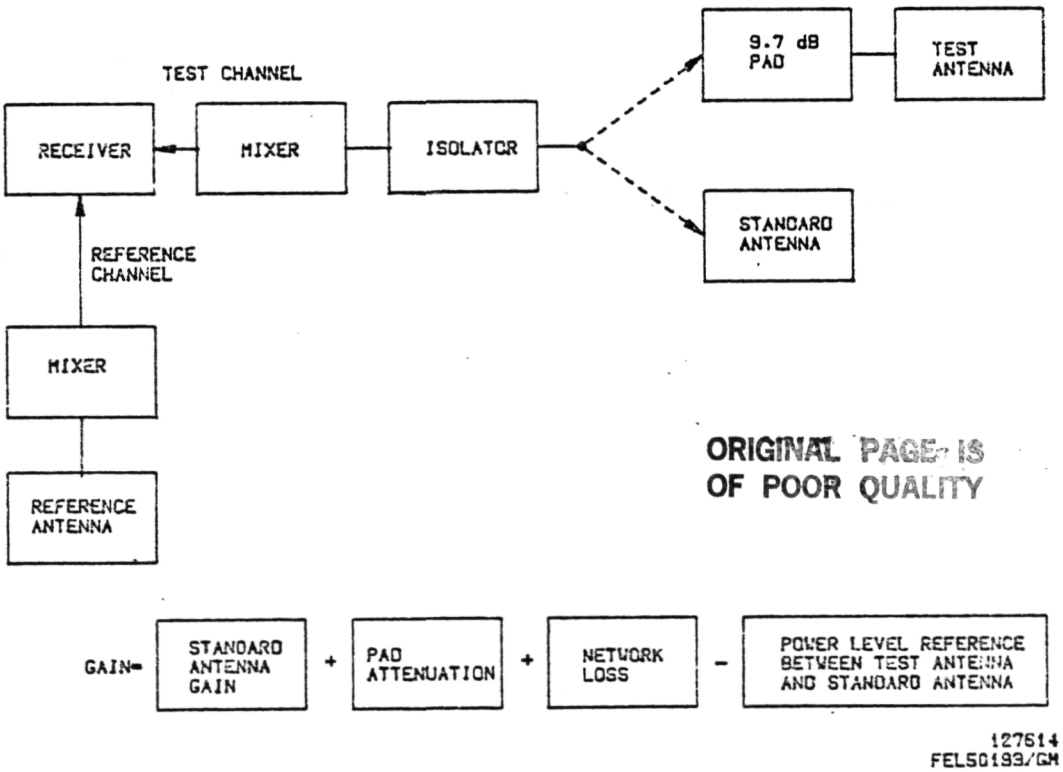

Figure 5.22 Gain Measurements Schematic Diagram

Table 5.2

Measured and Calculated Gains for Beams #9 & #109
Horizontal Polarization

Array Positions (In Pitches)	GAIN (dB)					
(X,Y)	Single Beam (#109)			7-Horn Cluster (#9)		
	C	M	D	C	M	D
(0,0)	53.29	53.04	0.25	55.16	54.89	0.27
(14,10)	53.35	52.94	0.41	54.82	54.19	0.63
(14,-10)	53.32	52.92	0.40	54.75	54.29	0.46
(-14,10)	52.10	51.99	0.11	54.09	53.74	0.35
(-14,-10)	52.00	51.92	0.08	54.00	53.92	0.08

C = Calculated M = Measured D = C - M

Table 5.3

Measured and Calculated Gains For Beams #9 & #109
Vertical Polarization

Array Positions (In Pitches)	Gain (dB)					
	Single Beam (#109)			7-Horn Cluster (#9)		
	C	M	D	C	M	D
(0,0)	53.06	53.07	-0.01	54.93	54.99	-0.06
(14,10)	53.15	52.89	0.26	54.72	54.25	0.47
(14,-10)	53.14	52.81	0.33	54.67	54.22	-0.45
(-14,10)	52.07	52.13	-0.06	54.08	53.93	0.15
(-14,-10)	52.00	51.85	0.15	54.02	53.93	0.09

C = Calculated M = Measured D = C-M

As a summary, we have the following conclusions:

The measured and calculated single-horn secondary patterns have excellent agreements.

The measured and calculated seven-horn cluster secondary patterns are also quite consistent, with the following variations for measured patterns.

(1) Azimuth Patterns show slightly higher sidelobes

(2) Elevation Patterns have slightly broader mainbeam

The variations could be caused by ground reflections, signal fluctutations, minor edge scattering, and inaccurate VPD & VPS settign (due to finite bits of VPS and VPD).

The measured patterns show only small sensitivity to frequency change.

The measured cross-pol patterns indicate that the worst cross-pol level for all patterns is about 32 dB below the co-pol peak.

The gain measurements for both single horn and 7-horn cluster are within 0.5 dB of the calculated values for all array positions.

Appendix A

Task Report Compliation

As required by the contract, detailed technical reports were submitted for Tasks I,II, IV, and VIII. These reports cover development of operational and demonstration concepts, breadboard development of critical components, and POC model testing. Abstracts for each of these task reports follow.

TASK I- DEVELOPMENT OF OPERATIONAL MBA SYSTEM CONCEPTS

The system requirements for 18 trunk beams and 6 scanning spot beams covering continental U.S. are reviewed and analyzed in detail, leading to the definition of a pair of dual shaped-surface reflector antennas for transmitting and receiving. The general arrangement with 2 antennas was selected by studying the features of spacecraft configurations using 1 to 4 antennas.

The dual shaped-surface reflectors resulted from optics design trade-offs where comparisons were made to four conventional offest reflector antennas:

- Single parabolic reflector with cylindrical feed.
- Cassegrain reflector pair with flat feed.
- Schwarzschild reflector pair with flat feed.
- Gregorian, Abbe' corrected, with a curved feed surface.

None of these conventional systems could provide the required wide scan angle without excessive pattern distortion and this led to the selection of dual shaped-surface reflectors. These reflector surfaces are adjusted to minimized path-length variation for feeds that cover the required area. The final design, C41.2, has a maximum calculated path-length error of 0.10 wavelength.

Calculated beams using 7-element feed clusters with this C41.2 design meet all specification requirements.

A unique beamforming network utilizing ferrite switches, phase shifters and power dividers was devised for the scan beam. The trunk beams, utilizing up to 13 horns each, are connected through diplexers and orthomode junctions as required to provide the required isolation.

Detailed design and performnace analyses for the MBA system showing overall compliance are made. These include contour plots for several cities, physical network configurations and weight-volume estimates.

Task II - ANTENNA SYSTEM CONCEPT FOR DEMONSTRATION SATELLITE

The results developed for the operational satellite in Task I are modified to fit the requirements of a demonstration satellite as described in the Statement-of-Work. In fact, two demonstration satellite versions, an SOW compliant version and a non-compliant, but less complex, version are presented. Weight and volume estimates are presented for both MBA versions. A recommendation is made that the non-compliant version be adopted for the demonstration model.

TASK IV - BREADBOARD DEVELOPMENT OF CRITICAL COMPONENTS

All new components required for the POC model were developed in breadboard form in this task. Examples of the passive wavewguide components; orthomode junctions, diplexer, feedhorn, and various waveguide bends were designed and tested.

A major development was for ferrite waveguide components; switches, phase shifters, and power dividers. This development, carried out by Electromagnetic Sciences of Atlanta, Georgia, included the electronic drivers and control circuits as well as the ferrite components themselves. Major testing was done at EMS, but some spot testing was done at FACC.

Photographs, test data, and detailed discussions are included for all components in the report.

TASK VIII - POC MODEL TESTING AND ANALYSIS

This report covers the POC model testing and analysis except for quality control testing that was done as a part of Task VII and was reproted in the Task VII Review.

The primary goal of the test program has been to measure and anlayze the MBA system performance characteristics; beamshape, sidelobe levels, gain, and pointing direction. For a reasonable understanding of the system limitations and to actually set the system up it was essential to also carry out extensive measurements on the networks and arrays subsystems.

To provide a reasonable representation of the pattern measurements for the various beam positions a large number of patterns, primary and secondary, are presented. There is far too much data to be included in a single volume so the material is presented in three volumes, one for the written descriptive material, a second volume for the primary pattern measurements and a third volume for the secondary pattern measurements.

Appendix B

Bibliography

Reference Number		Date
1	Major Review Number 1	11-80
2	Major Review Number 2	4-81
3	Industry Briefing	5-81
4	Major Review Number 3	9-81
5	Final Report for FACC 20 GHz BFN Switch Control Elements	9-81
6	Top Level Test Plan	12-81
7	Major Review Number 4	5-82
8	Task 1 & Task 2 Report	5-82
9	Preliminary Test Plan	5-82
10	Operating Manual for Central Electronics by Electronagnetic Sciences, Inc.	11-82
11	Final Report by Electromagnetic Sciences, Inc.	11-82
12	Test Plan II	2-82
13	Test VII POC Model Fabrication Review	4-83
14	Final Report and Data Summary by Tinsley Laboratories	4-83
15	Task 8 Report, POC Model Testing and Analysis, Vol. 1, II, & III	11-83
16	Potential Technology Studies	5-83

ORIGINAL PAGE IS
OF POOR QUALITY

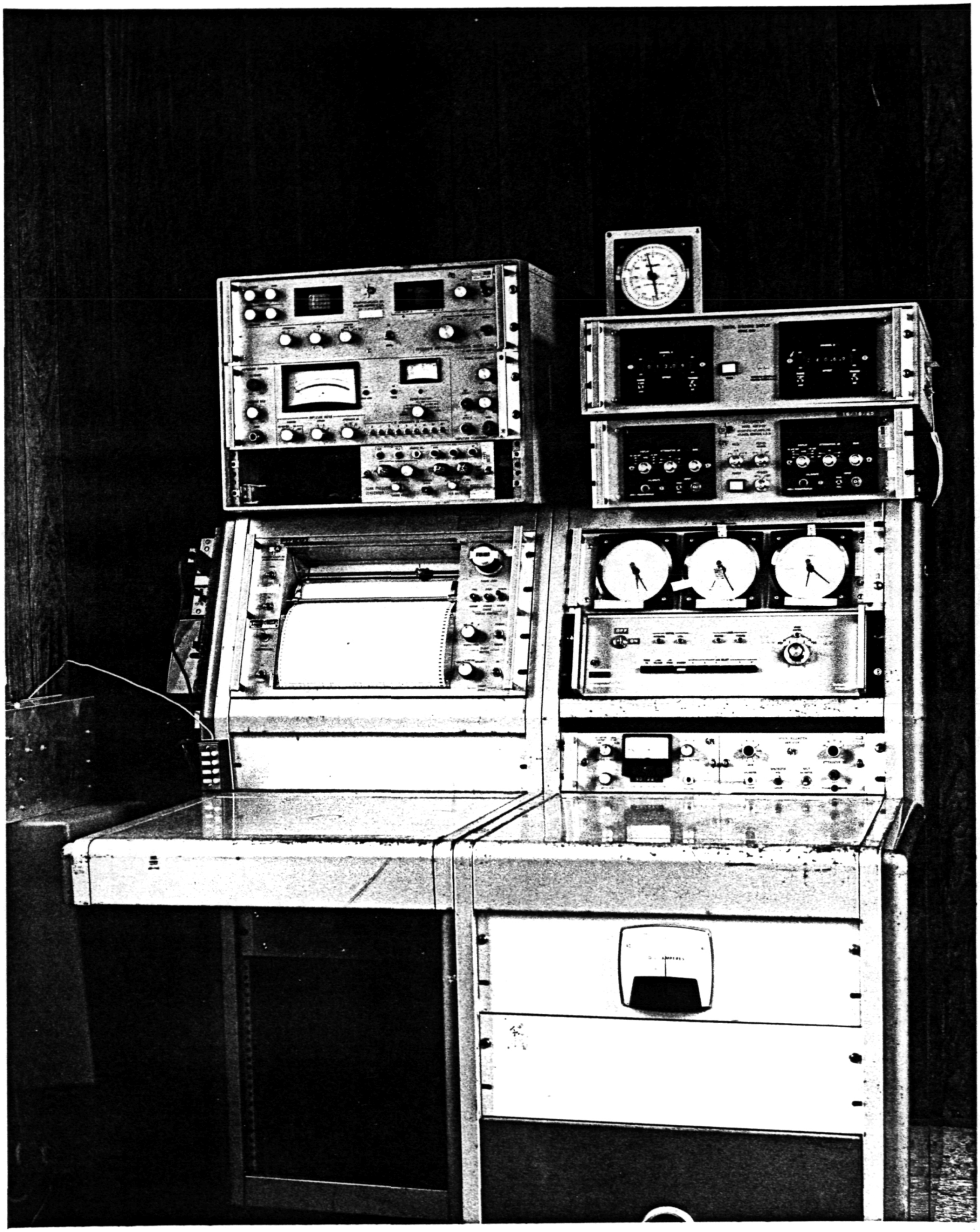

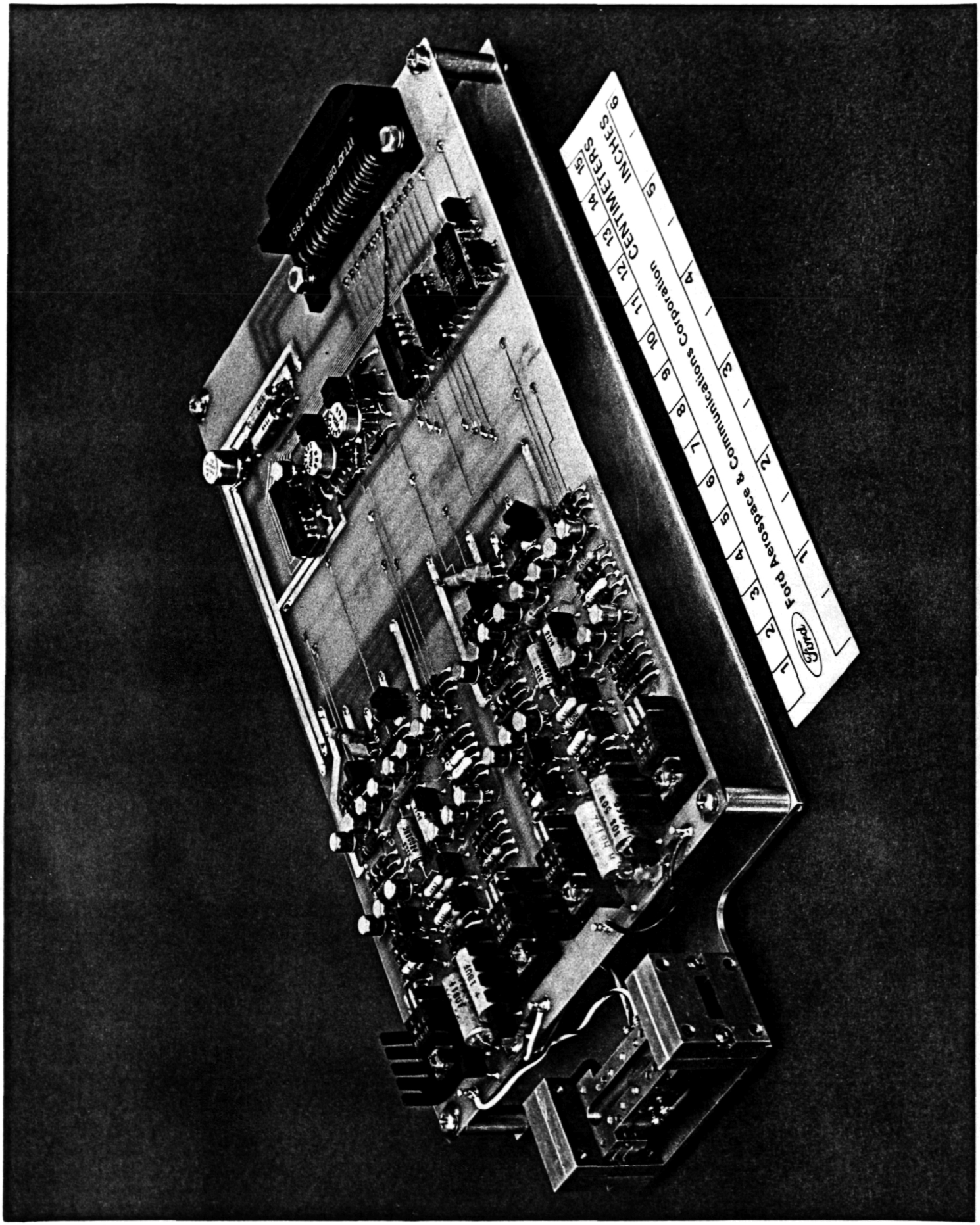

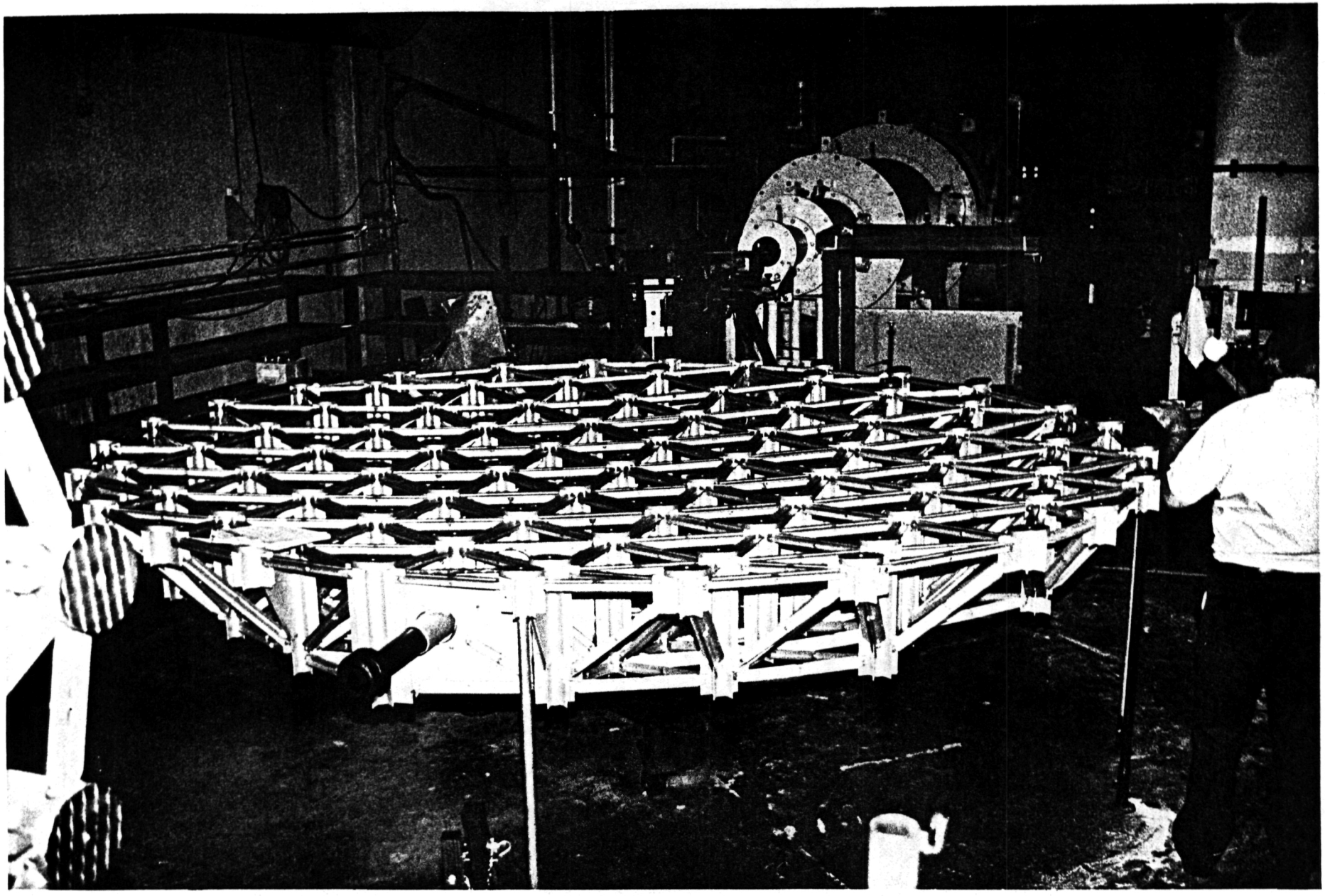

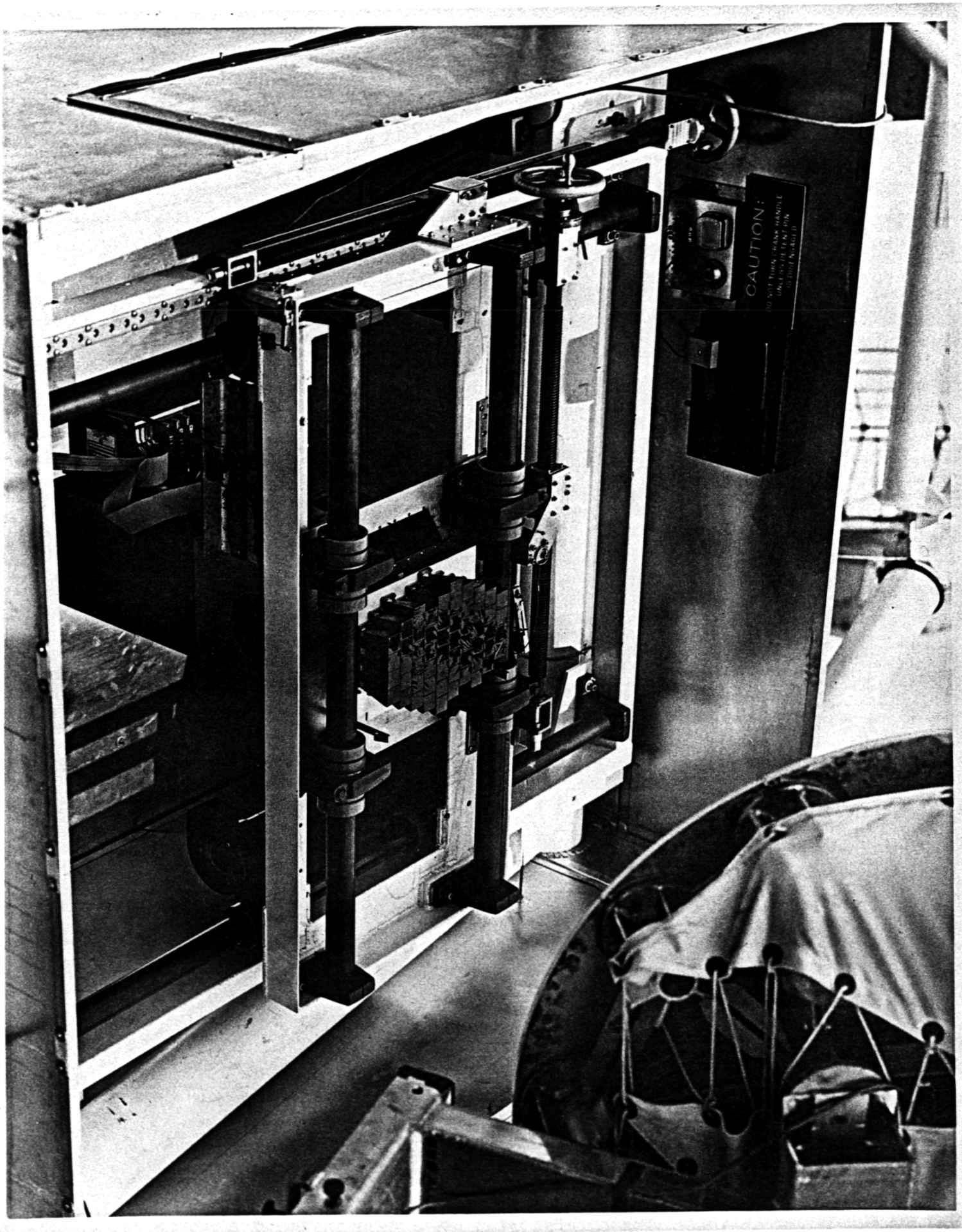

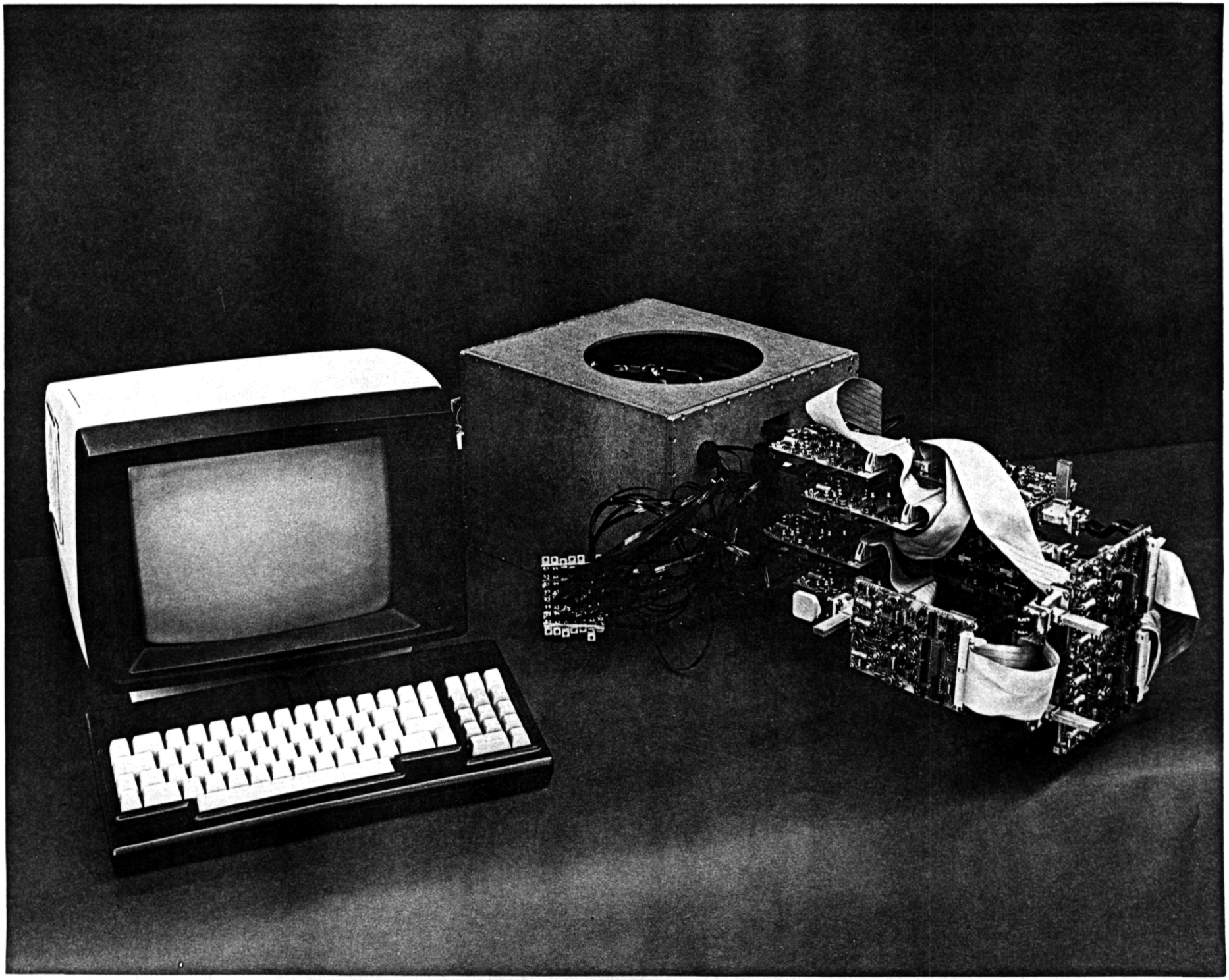

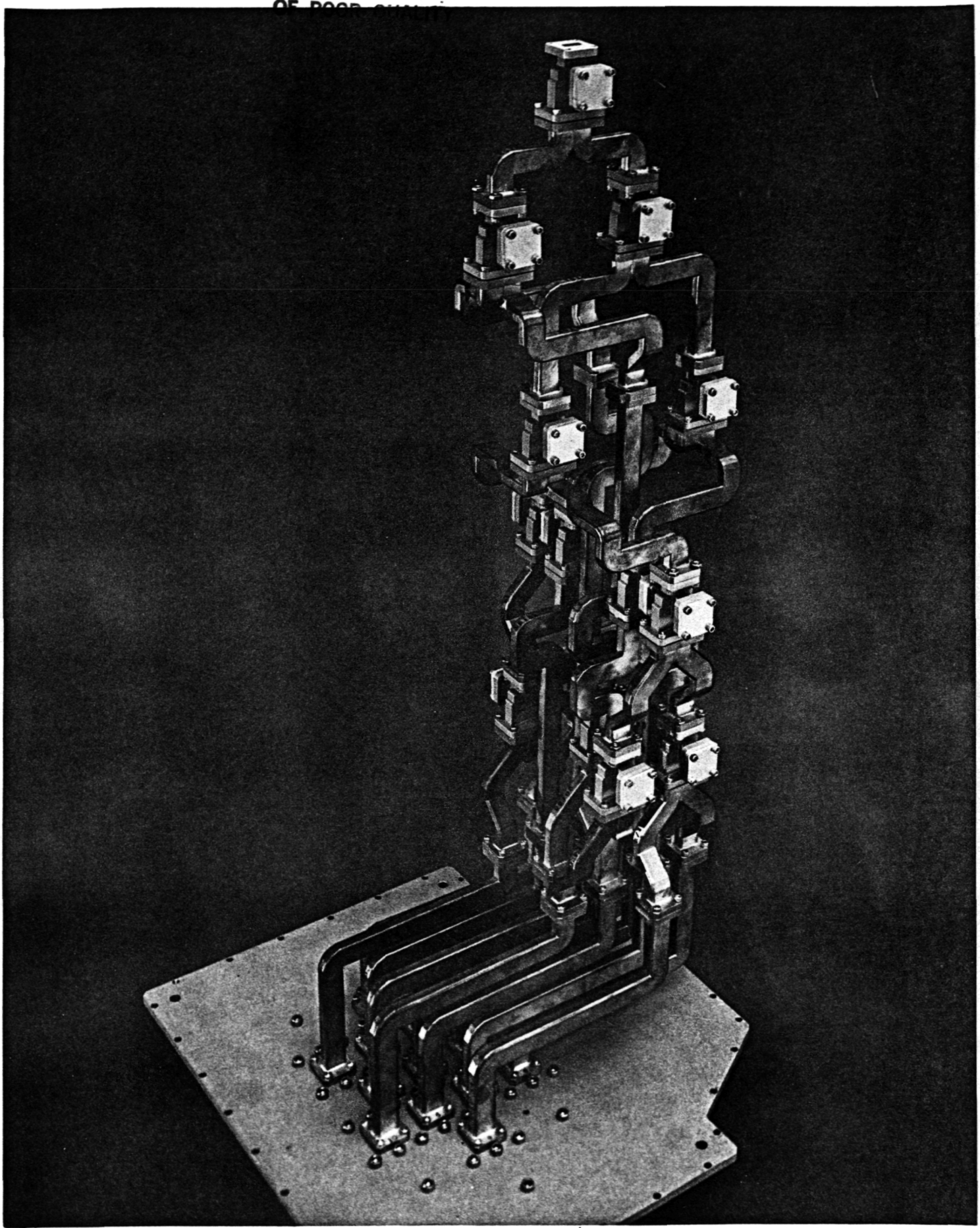

1. Report No.	2. Government Accession No.	3. Recipient's Catalog No.
NASA CR-174654		

4. Title and Subtitle	5. Report Date
Spacecraft Multibeam Antenna System for 30/20 GHz	January 1984
	6. Performing Organization Code

7. Author(s)	8. Performing Organization Report No.
T. E. Roberts and W. F. Scott	WDL-TR10138
	10. Work Unit No.

9. Performing Organization Name and Address	11. Contract or Grant No.
Ford Aerospace and Communications Corp. Western Development Laboratories Div. Palo Alto, California 94303	NAS 3-22498
	13. Type of Report and Period Covered
12. Sponsoring Agency Name and Address	Contract Report
National Aeronautics and Space Adminstration Washington, D.C. 20546	14. Sponsoring Agency Code
	650-60-20

15. Supplementary Notes

Final report. Project Manager, Royce W. Myhre, Space Communications Division, NASA Lewis Research Center, Cleveland, Ohio 44135.

16. Abstract

This final report describes the major technical tasks that led to the definitions of Operational and Demonstration Multiple Beam Antenna Flight Systems and a Proof of Concept Model. Features of the POC Model and its measured performance are presented in detail. Similar MBA's are proposed for transmitting and receiving with the POC Model representing the 20 GHz transmitting antenna. This POC MBA is a dual shaped-surface reflector system utilizing a movable feed array to simulate complete CONUS coverage. The beam forming network utilizes ferrite components for switching from one beam to another. Measured results for components, subsystems and the complete MBA confirm the feasibility of the approach and also show excellent correlation with calculated values.

17. Key Words (Suggested by Author(s))	18. Distribution Statement
Satellite communications systems Ka band communications satellites Multiple beam antennas	UNCLASSIFIED UNLIMITED

19. Security Classif. (of this report)	20. Security Classif. (of this
Unclassified	Unclassified